

A unified framework for structured low-rank matrix learning

Pratik Jawanpuria
Amazon.com
jawanpur@amazon.com

Bamdev Mishra
Amazon.com
bamdevm@amazon.com

Abstract

We propose a novel optimization framework for learning a low-rank matrix which is also constrained to lie in a linear subspace. Exploiting the duality theory, we present a factorization that decouples the low-rank and structural constraints onto separate factors. The optimization problem is formulated on the Riemannian spectrahedron manifold, where the Riemannian framework allows to develop computationally efficient conjugate gradient and trust-region algorithms. Our approach easily accommodates popular non-smooth loss functions, e.g., ℓ_1 -loss, and our algorithms are scalable to large-scale problem instances. The numerical comparisons show that our algorithms outperform state-of-the-art in standard, robust, and non-negative matrix completion, Hankel matrix learning, and multi-task feature learning problems on various benchmarks.

1 Introduction

Our focus in this paper is on learning structured low-rank matrices with the formulation

$$\begin{aligned} \min_{\mathbf{W} \in \mathbb{R}^{d \times T}} \quad & \frac{1}{2}R(\mathbf{W}) + CL(\mathbf{W}, \mathbf{Y}), \\ \text{subject to} \quad & \mathbf{W} \in \mathcal{D}, \end{aligned} \tag{1}$$

where $\mathbf{Y} \in \mathbb{R}^{d \times T}$ is a given matrix, $L : \mathbb{R}^{d \times T} \times \mathbb{R}^{d \times T} \rightarrow \mathbb{R}$ is a loss function, R is a low-rank promoting regularizer, $C > 0$ is the cost parameter, and \mathcal{D} is the *linear* subspace corresponding to structural constraints.

Low-rank matrices are commonly learned in several machine learning applications such as matrix completion (Candès & Recht, 2009), multi-task learning (Argyriou et al., 2008; Amit et al., 2007), multivariate regression (Yuan et al., 2007; Journée et al., 2010), to name a few. In addition to the low-rank constraint, other structural constraints may exist, e.g., entry-wise *non-negative/bounded* constraints (Marecek et al., 2017; Kannan et al., 2012; Fang et al., 2017). Several linear dynamical system models require learning a low-rank *Hankel* matrix (Fazel et al., 2013; Markovsky & Usevich, 2013). A Hankel matrix has the structural constraint that all its anti-diagonal entries are the same. In robust matrix completion (Candès & Plan, 2009) and robust PCA (Wright et al., 2009) problems, the matrix is learned as a superimposition of a low-rank matrix and a sparse matrix. This sparse structure is modeled effectively by choosing the loss function as the ℓ_1 -loss (Cambier & Absil, 2016). Low-rank 1-bit matrix completion solvers employ the *logistic* loss function (Davenport et al., 2014; Bhaskar & Javanmard, 2015).

We propose a *generic* framework to the structured low-rank matrix learning problem (1) that is well suited for handling a variety of loss functions L (e.g., ℓ_1 -loss function), structural constraints \mathcal{D} , and is scalable for large-scale problem instances. Using the duality theory, we present a novel modeling of structured low-rank matrix \mathbf{W} as $\mathbf{W} = \mathbf{U}\mathbf{U}^\top(\mathbf{Z} + \mathbf{A})$, where $\mathbf{U} \in \mathbb{R}^{d \times r}$ and $\mathbf{Z}, \mathbf{A} \in \mathbb{R}^{d \times T}$. Our factorization naturally decouples the low-rank and structural constraints on \mathbf{W} . The

low-rank of \mathbf{W} is enforced with \mathbf{U} , the structural constraint is modeled by \mathbf{A} , and the loss function specific structure is modeled by \mathbf{Z} . The separation of low-rank and structural constraints onto separate factors makes the optimization conceptually simpler. To the best of our knowledge, such a decoupling of constraints has not been studied in the existing structured low-rank matrix learning literature (Fazel et al., 2013; Markovsky & Usevich, 2013; Cambier & Absil, 2016; Yu et al., 2014).

Our approach leads to an optimization problem on the *Riemannian spectrahedron* manifold. We exploit the Riemannian framework to develop computationally efficient conjugate gradient (first-order) and trust-region (second-order) algorithms.

The proposed algorithms outperform state-of-the-art in standard, robust and non-negative matrix completion problems as well as low-rank Hankel matrix learning applications. Our algorithms readily scale to the Netflix data set, even for the non-smooth ℓ_1 -loss and ϵ -SVR (ϵ -insensitive support vector regression) loss functions.

The main contributions of the paper are:

- we propose a novel factorization $\mathbf{W} = \mathbf{U}\mathbf{U}^\top(\mathbf{Z} + \mathbf{A})$ for modeling structured low-rank matrices.
- we present a unified framework to learn structured low-rank matrix for several applications.
- we obtain state-of-the-art performance, in both generalization error and computational efficiency, across applications.

The outline of the paper is as follows. We introduce our structured low-rank matrix learning framework in Section 3. Section 4 presents our optimization methodology. In Section 5, we discuss specialized formulations resulting from our framework for various matrix completion problems, Hankel matrix learning and multi-task feature learning. The empirical results are presented in Section A.5. The proofs of all the theorems as well as additional experiments are provided in the supplementary material. We begin by discussing the related works in the next section.

The proofs of all the theorems as well as additional experiments are provided in the supplementary section. The Matlab codes are available on <https://pratikjawanpuria.com/>.

2 Related work

Matrix completion: Cai et al. (2010); Toh & Yun (2010); Hsieh & Olsen (2014) propose singular value thresholding and active learning algorithms for (1) with $R(\mathbf{W}) = \|\mathbf{W}\|_*$ and without the constraint $\mathbf{W} \in \mathcal{D}$.

Fixed-rank approaches (Boumal & Absil, 2011; Wen et al., 2012; Mishra & Sepulchre, 2014; Tan et al., 2016) learn a low-rank matrix by fixing the rank explicitly. They differ in the scheme of factorization and the algorithm to solve (1). Wen et al. (2012) propose alternate least-squares algorithms (and variants) for the matrix completion problem. Several works (Vandereycken, 2013; Boumal & Absil, 2015) exploit the Riemannian geometry of fixed-rank matrices and propose a number of first- and second-order algorithms.

Robust matrix completion: Robust versions of the matrix completion problem have been studied in several works (Candès et al., 2011; He et al., 2012; Yan et al., 2013; Cambier & Absil, 2016). Candès et al. (2011) model the robust matrix completion problem as a convex program with separate low-rank and sparse constraints. He et al. (2012) propose to use ℓ_1 -loss as the loss function and impose only the low-rank constraint. They propose an online algorithm that learns a low-dimensional subspace. Cambier & Absil (2016) build on this and employ the pseudo-Huber loss as a proxy for the non-smooth ℓ_1 -loss. They develop a large-scale Riemannian conjugate gradient algorithm.

Non-negative matrix completion: Certain recommender system and image completion based applications desire matrix completion with non-negative entries (Kannan et al., 2012; Sun &

Mazumder, 2013; Tsagkatakis et al., 2016; Fang et al., 2017). Kannan et al. (2012) present a coordinate descent algorithm that learns a low-rank factorization. Recently, Fang et al. (2017) propose a large-scale alternating direction method of multipliers (ADMM) algorithm.

Hankel matrix learning: Fazel et al. (2013) use $R(\mathbf{W}) = \|\mathbf{W}\|_*$ in (1) to learn a low-rank Hankel matrix (enforced by \mathcal{D}) with the ADMM approaches. Yu et al. (2014) also exploit $\|\mathbf{W}\|_*$ as low-rank enforcing regularizer for learning Hankel matrices, but relax the structural constraint with a penalty term in the objective function. They discuss a generalized gradient algorithm. Instead of employing $R(\mathbf{W})$ in (1), Markovsky & Usvich (2013) learn a Hankel matrix by fixing the rank *a priori* and strictly enforcing the structural constraints.

Multi-task feature learning: The goal in multi-task feature learning (MTFL) is to jointly learn a low-dimensional latent feature representation common across several classification/regression problems (tasks). Existing works (Argyriou et al., 2008; Ji & Ye, 2009; Zhang & Yeung, 2010; Ciliberto et al., 2015) have employed $R(\mathbf{W}) = \|\mathbf{W}\|_*^2$ or $\|\mathbf{W}\|_*$. The optimization approaches explored include alternate minimization (Argyriou et al., 2008; Zhang & Yeung, 2010), accelerated gradient descent (Ji & Ye, 2009) and block coordinate descent (Ciliberto et al., 2015).

3 Novel formulation for structured low-rank matrix learning

We present our formulations and derivations for the problem of learning a structured low-rank matrix \mathbf{W} close to a given matrix \mathbf{Y} . The linear subspace \mathcal{D} in problem (1) is represented as $\mathcal{D} := \{\mathbf{W} : \mathcal{A}(\mathbf{W}) = \mathbf{0}\}$, where $\mathcal{A} : \mathbb{R}^{d \times T} \rightarrow \mathbb{R}^n$ is a linear map. The set of $d \times d$ positive semi-definite matrices with unit trace is denoted by \mathcal{P}^d . The pseudoinverse of a matrix Θ is represented as Θ^\dagger .

We begin with a well-known variational characterization of the squared trace norm regularizer.

Lemma 1. [Theorem 4.1 in (Argyriou et al., 2006)] Let $\text{range}(\Theta) = \{\Theta z : z \in \mathbb{R}^d\}$. The following results holds:

$$\|\mathbf{W}\|_*^2 = \min_{\Theta \in \mathcal{P}^d, \text{range}(\mathbf{W}) \subseteq \text{range}(\Theta)} \langle \Theta^\dagger \mathbf{W}, \mathbf{W} \rangle. \quad (2)$$

For a given \mathbf{W} matrix, the optimal $\bar{\Theta} = \sqrt{\mathbf{W}\mathbf{W}^\top} / \text{trace}(\sqrt{\mathbf{W}\mathbf{W}^\top})$.

Based on the above result, we study the following variant of problem (1) by taking the low-rank regularizer $R(\mathbf{W}) = \|\mathbf{W}\|_*^2$, i.e.,

$$\begin{aligned} \min_{\Theta \in \mathcal{P}^d} \min_{\mathbf{W} \in \mathbb{R}^{d \times T}} \quad & \frac{1}{2} \langle \Theta^\dagger \mathbf{W}, \mathbf{W} \rangle + CL(\mathbf{Y}, \mathbf{W}) \\ \text{subject to : } & \mathcal{A}(\mathbf{W}) = \mathbf{0}, \text{ range}(\mathbf{W}) \subseteq \text{range}(\Theta). \end{aligned} \quad (3)$$

It should be noted that the Θ learned in (3) is a low-rank matrix because it is positive semi-definite with $\text{trace}(\Theta) = 1$ constraint. In addition, Lemma 1 guarantees that the rank of Θ and \mathbf{W} are equal at optimality. Hence, in problem (3), the low-rank constraint on \mathbf{W} is *transferred* to Θ . In the following, we derive and analyze a dual formulation of (3) that is suitable in large-scale structured matrix learning.

3.1 Dual formulation

The dual formulation of (3), presented in the next theorem, provides further insights into the optimization problem (3) and its optimal solution.

Theorem 1. Let L^* be the Fenchel conjugate function of the loss: $L : \mathbb{R}^{d \times T} \rightarrow \mathbb{R}$, $v \mapsto L(\mathbf{Y}, v)$. The dual problem of (3) with respect to \mathbf{W} is

$$\min_{\Theta \in \mathcal{P}^d} \max_{\mathbf{Z} \in \mathbb{R}^{d \times T}, s \in \mathbb{R}^n} f(\Theta, \mathbf{Z}, s), \quad (4)$$

where the function f is defined as

$$f(\Theta, \mathbf{Z}, s) := -CL^*\left(\frac{-\mathbf{Z}}{C}\right) - \frac{1}{2} \langle \Theta(\mathbf{Z} + \mathcal{A}^*(s)), \mathbf{Z} + \mathcal{A}^*(s) \rangle,$$

and $\mathcal{A}^* : \mathbb{R}^n \rightarrow \mathbb{R}^{d \times T}$ is the adjoint of \mathcal{A} .

Furthermore, let $\{\bar{\Theta}, \bar{\mathbf{Z}}, \bar{s}\}$ be an optimal solution of (4), then the optimal solution $\bar{\mathbf{W}}$ of (3) is given by $\bar{\mathbf{W}} = \bar{\Theta}(\bar{\mathbf{Z}} + \mathcal{A}^*(\bar{s}))$.

Theorem 1 has the following implications. The optimal $\bar{\mathbf{W}}$ is a product of two terms, $\bar{\Theta}$ and $\bar{\mathbf{Z}} + \mathcal{A}^*(\bar{s})$. The low-rank constraint is enforced through $\bar{\Theta}$, the loss-specific structure (encoded in L^*) is enforced through $\bar{\mathbf{Z}}$, and the structural constraint is enforced through $\mathcal{A}^*(\bar{s})$. Overall, such a decoupling of constraints onto separate variables facilitates the use of simpler optimization techniques as compared to the case where all the constraints are enforced on a single variable.

As discussed earlier, an optimal $\bar{\Theta}$ of (4) is a low-rank positive semi-definite matrix. However, an algorithm for (4) need not produce intermediate iterates that are low rank. For large-scale optimization, this observation as well as other computational efficiency concerns motivate a fixed-rank parameterization of Θ as discussed in the following section.

3.2 Fixed-rank parameterization

We model $\Theta \in \mathcal{P}^d$ as a rank r matrix as follows: $\Theta = \mathbf{U}\mathbf{U}^\top$, where $\mathbf{U} \in \mathbb{R}^{d \times r}$ and $\|\mathbf{U}\|_F = 1$. The proposed modeling has several benefits in large-scale low-rank matrix learning problems, where $r \ll \min\{d, T\}$ is a common setting. *First*, the parameterization ensures that $\Theta \in \mathcal{P}^d$ constraint is always satisfied. This saves the costly projection operations to ensure $\Theta \in \mathcal{P}^d$. Enforcing $\|\mathbf{U}\|_F = 1$ constraint costs $O(rd)$. *Second*, the dimension of the search space of problem (4) with $\Theta = \mathbf{U}\mathbf{U}^\top$ is $rd - 1 - r(r - 1)/2$, which is much lower than the dimension $(d(d + 1)/2 - 1)$ of $\Theta \in \mathcal{P}^d$. By restricting the search space for Θ , we gain computational efficiency. *Third*, increasing the parameter C in (4) and (3) promotes low training error but high rank of the solution, and vice-versa. The proposed fixed-rank parameterization decouples this trade-off.

Instead of solving a minimax objective directly, as in (4), we solve a minimization problem after incorporating the $\Theta = \mathbf{U}\mathbf{U}^\top$ parameterization as follows:

$$\min_{\mathbf{U} \in \mathbb{R}^{d \times r}, \|\mathbf{U}\|_F = 1} g(\mathbf{U}), \quad (5)$$

where the function g is defined as

$$g(\mathbf{U}) := \max_{\mathbf{Z} \in \mathbb{R}^{d \times T}, s \in \mathbb{R}^n} -CL^*(-\mathbf{Z}/C) - \frac{1}{2} \left\| \mathbf{U}^\top (\mathbf{Z} + \mathcal{A}^*(s)) \right\|_F^2. \quad (6)$$

An important outcome of the above modeling is that the *expression* for the gradient of $g(\mathbf{U})$ in (5) is *independent* of the application at hand (refer Lemma 2). The application specific information in (6) is encoded only through the *values* of variables \mathbf{Z} and s , which are used to compute the gradient of $g(\mathbf{U})$. This allows the development of a *unified* optimization framework for several low-rank matrix

Algorithm 1 Proposed first- and second-order algorithms for (5)

Input: \mathbf{Y} , rank r , regularization parameter C .

Initialize $\mathbf{U} \in \mathcal{S}_r^d$.

repeat

1: Solve for $\{\mathbf{Z}, s\}$ by computing $g(\mathbf{U})$ in (6). Section 5 discusses solvers for specific applications.

2: Compute $\nabla_{\mathbf{U}}g(\mathbf{U})$ as given in Lemma 2.

3: **Riemannian CG step:** compute a conjugate direction \mathbf{V} and step size α using Armijo line search. It makes use of $\nabla_{\mathbf{U}}g(\mathbf{U})$.

3: **Riemannian TR step:** compute a search direction \mathbf{V} which minimizes the trust region sub-problem. It makes use of $\nabla_{\mathbf{U}}g(\mathbf{U})$ and its directional derivative. Step size $\alpha = 1$.

4: Update $\mathbf{U} = (\mathbf{U} + \alpha\mathbf{V})/\|\mathbf{U} + \alpha\mathbf{V}\|_F$ (retraction step)

until convergence

Output: $\{\mathbf{U}, \mathbf{Z}, s\}$ and $\mathbf{W} = \mathbf{U}\mathbf{U}^\top(\mathbf{Z} + \mathcal{A}^*(s))$.

learning problems such as Hankel matrix learning, non-negative matrix completion, standard- and robust-matrix completion, to name a few. Finally, the matrix \mathbf{W} is learned as $\mathbf{U}\mathbf{U}^\top(\mathbf{Z} + \mathcal{A}^*(s))$.

We end this section by providing the duality gap optimality criterion of any *feasible* solution $\hat{\mathbf{U}}$ of (5) with respect to (4).

Theorem 2. Let $\hat{\mathbf{U}}$ be a feasible solution of (5) and $\{\hat{\mathbf{Z}}, \hat{s}\}$ be an optimal solution of the convex problem in (6) at $\hat{\mathbf{U}}$. In addition, let σ_1 be the maximum singular of the matrix $\hat{\mathbf{Z}} + \mathcal{A}^*(\hat{s})$. A candidate solution for (4) is $\{\hat{\Theta}, \hat{\mathbf{Z}}, \hat{s}\}$, where $\hat{\Theta} = \hat{\mathbf{U}}\hat{\mathbf{U}}^\top$. The duality gap (Δ) associated with $\{\hat{\Theta}, \hat{\mathbf{Z}}, \hat{s}\}$ is given by

$$\Delta = \frac{1}{2} \left(\sigma_1^2 - \left\| \hat{\mathbf{U}}^\top (\hat{\mathbf{Z}} + \mathcal{A}^*(\hat{s})) \right\|_F^2 \right).$$

The cost of computing σ_1 is computationally cheap as it requires only a few *power iteration* updates.

4 Optimization on spectrahedron manifold

The matrix \mathbf{U} lies in, what is popularly known as, the *spectrahedron* manifold $\mathcal{S}_r^d := \{\mathbf{U} \in \mathbb{R}^{d \times r} : \|\mathbf{U}\|_F = 1\}$. Specifically, the spectrahedron manifold has the structure of a compact Riemannian quotient manifold (Journée et al., 2010). The quotient structure takes the rotational invariance of the constraint $\|\mathbf{U}\|_F = 1$ into account. The Riemannian optimization framework embeds the constraint $\mathbf{U} \in \mathcal{S}_r^d$ into the search space, conceptually translating the constrained optimization problem (5) into an *unconstrained* optimization over the spectrahedron manifold. The Riemannian optimization framework generalizes various classical first- and second-order Euclidean algorithms (e.g., the conjugate gradients and trust region algorithms) to manifolds and provide concrete convergence guarantees (Edelman et al., 1998; Absil et al., 2008; Journée et al., 2010; Sato & Iwai, 2013; Zhang et al., 2016; Sato et al., 2017). In particular, Absil et al. (2008) provide a systematic way of implementing Riemannian conjugate gradient (CG) and trust region (TR) algorithms.

We implement the Riemannian conjugate gradient (CG) and trust-region (TR) algorithms for (5). These require the notions of the *Riemannian gradient* (first-order derivative of the objective function on the manifold), *Riemannian Hessian* along a search direction (the *covariant* derivative of the Riemannian gradient along a tangential direction on the manifold), and the *retraction* operator (that ensures that we always stay on the manifold). The Riemannian gradient and Hessian notions require computations of the standard (Euclidean) gradient and the directional derivative of this gradient along a given search direction, which are expressed in the following lemma.

Lemma 2. Let $\{\hat{\mathbf{Z}}, \hat{s}\}$ be an optimal solution of the convex problem (6) at \mathbf{U} . Then, the gradient of $g(\mathbf{U})$ is given by

$$\nabla_{\mathbf{U}}g(\mathbf{U}) = -(\hat{\mathbf{Z}} + \mathcal{A}^*(\hat{s}))(\hat{\mathbf{Z}} + \mathcal{A}^*(\hat{s}))^\top \mathbf{U}.$$

Let $D\nabla_{\mathbf{U}}g(\mathbf{U})[\mathbf{V}]$ denote the directional derivative of the gradient $\nabla_{\mathbf{U}}g(\mathbf{U})$ along $\mathbf{V} \in \mathbb{R}^{d \times r}$. Let $\{\dot{\mathbf{Z}}, \dot{s}\}$ denote the directional derivative of $\{\mathbf{Z}, s\}$ along \mathbf{V} at $\{\hat{\mathbf{Z}}, \hat{s}\}$. Then,

$$\begin{aligned} D\nabla_{\mathbf{U}}g(\mathbf{U})[\mathbf{V}] &= (\dot{\mathbf{Z}} + \mathcal{A}^*(\dot{s}))(\hat{\mathbf{Z}} + \mathcal{A}^*(\hat{s}))^\top \mathbf{U} \\ &\quad + (\hat{\mathbf{Z}} + \mathcal{A}^*(\hat{s})) \left((\dot{\mathbf{Z}} + \mathcal{A}^*(\dot{s}))^\top \mathbf{U} - (\hat{\mathbf{Z}} + \mathcal{A}^*(\hat{s}))^\top \mathbf{V} \right). \end{aligned}$$

In various applications such as matrix completion and multi-task feature learning, both the gradient $\nabla_{\mathbf{U}}g(\mathbf{U})$ and its directional derivation $D\nabla_{\mathbf{U}}g(\mathbf{U})[\mathbf{V}]$ can be computed via closed form expressions.

Riemannian CG algorithm: It computes the Riemannian *conjugate* gradient direction by employing the first-order information $\nabla_{\mathbf{U}}g(\mathbf{U})$ (Lemma 2). We perform *Armijo* line search on \mathcal{S}_r^d to compute a step-size that sufficiently decreases $g(\mathbf{U})$ on the manifold. We update along the conjugate direction with the step-size by *retraction*.

Riemannian TR algorithm: It solves a Riemannian trust-region *sub-problem* (in a neighborhood) at every iteration. Solving the trust-region sub-problem leads to a search direction that minimizes a *quadratic* model of $g(\mathbf{U})$ on the manifold. Solving this sub-problem does not require inverting the full Hessian of the objective function. It makes use of $\nabla_{\mathbf{U}}g(\mathbf{U})$ and its directional derivative $D\nabla_{\mathbf{U}}g(\mathbf{U})[\mathbf{V}]$ (Lemma 2).

Overall algorithm: Algorithm 1 summarizes the proposed first- and second-order algorithms for solving (5). Although we have focused on CG and TR algorithms for (5) in this paper, our approach can be readily extended to a stochastic setting, e.g., when $\mathcal{A}(\mathbf{W}) = \mathbf{0}$ imposes column-wise constraints and the columns are streamed one by one.

Computational complexity: The computational complexity of Algorithm 1 is the sum of the cost of manifold related operations and the cost of application specific ingredients. The spectrahedron manifold operations cost $O(dr + r^3)$. Section 5 discusses the application specific computational costs.

5 Specialized formulations for various problems

The overall problem (5) remains the same for various structured low-rank matrix learning problems. Depending on the constraints, the function $g(\mathbf{U})$ changes. Below we discuss the concrete formulations for popular applications.

5.1 Matrix completion

Given a partially observed matrix \mathbf{Y} at indices Ω , we learn the full matrix \mathbf{W} (Toh & Yun, 2010; Cai et al., 2010). Let Ω_t be the set of indices that are observed in y_t , the t^{th} column of \mathbf{Y} . Let $y_{t_{\Omega_t}}$ and \mathbf{U}_{Ω_t} represents the rows of y_t and \mathbf{U} , respectively, that correspond to the indices in Ω_t . Then, the function $g(\mathbf{U})$ in (6), for the standard low-rank matrix completion problem with square loss, is as follows:

$$g(\mathbf{U}) = \sum_{t=1}^T \max_{z_t \in \mathbb{R}^{|\Omega_t|}} z_t^\top y_{t_{\Omega_t}} - \frac{\|z_t\|^2}{4C} - \frac{\|\mathbf{U}_{\Omega_t}^\top z_t\|^2}{2}. \quad (7)$$

Problem (7) is a least-squares problem for each z_t and can be solved efficiently in closed-form by employing the Woodbury matrix-inversion identity. The computational cost of solving problem (7) is $O(|\Omega|r^2)$. Overall, the per-iteration computational cost of Algorithm 1 is $O(|\Omega|r^2 + dr + r^3)$. Problem (7) can be solved in parallel for each t , making it amenable to parallelization.

5.2 Robust matrix completion

The setting of this problem is same as the standard low-rank matrix completion problem, except that a *robust* loss function such as ℓ_1 -loss is employed instead of the square loss (Candès & Plan, 2009; He et al., 2012; Cambier & Absil, 2016). The function $g(\mathbf{U})$ specialized for the robust low-rank matrix completion problem with ℓ_1 -loss is as follows:

$$g(\mathbf{U}) = \sum_{t=1}^T \max_{z_t \in [-C, C]^{|\Omega_t|}} z_t^\top y_{t\Omega_t} - \frac{1}{2} \left\| \mathbf{U}_{\Omega_t}^\top z_t \right\|^2. \quad (8)$$

A dual coordinate descent algorithm (Ho & Lin, 2012) is employed to efficiently solve (8). The computational cost of solving problem (8) depends on the number of iterations of the dual coordinate descent algorithm. In particular, if k is the number of iterations, then the cost of computing $g(\mathbf{U})$ is $O(|\Omega|kr^2)$. In our experiments, we observe that a small value of k is sufficient to obtain a good approximation of (8). Overall, the per-iteration computational cost of Algorithm 1 is $O(|\Omega|kr^2 + dr + r^3)$.

Apart from the ℓ_1 -loss, we also experiment with the ϵ -SVR loss function (the results discussed in Section A.5).

5.3 Non-negative matrix completion

In this problem, the aim is to complete a partially observed matrix \mathbf{Y} with non-negative entries only. The function $g(\mathbf{U})$ specialized for non-negative low-rank matrix completion is as follows:

$$g(\mathbf{U}) = \sum_{t=1}^T \max_{z_t \in \mathbb{R}^{|\Omega_t|}, s_t \in [0, \infty)^d} z_t^\top y_{t\Omega_t} - \frac{\|z_t\|^2}{4C} - \frac{1}{2} \left\| \mathbf{U}_{\Omega_t}^\top z_t + \mathbf{U}^\top s_t \right\|^2. \quad (9)$$

We employ the non-negative least squares (NNLS) algorithm of Kim et al. (2013) to solve for the variable s_t in (9). In each iteration of NNLS, we solve for z_t in closed form. If k is the number of iterations of NNLS, then the cost of computing $g(\mathbf{U})$ is $O(dTkr + |\Omega|kr^2)$. Overall, the per-iteration computational cost of Algorithm 1 is $O(dTkr + |\Omega|kr^2 + dr + r^3)$. Similar to Section 5.2, a small value of k suffices for a good approximation to the solution of (9).

It should be noted that (9) is computationally challenging as it has dT entry-wise non-negativity constraints. In our initial experiments, we observe that the solution $[s_1, \dots, s_T]$ is highly sparse. For large-scale problems, we exploit this observation for an efficient implementation.

5.4 Hankel matrix learning

Hankel matrices have the structural constraint that its anti-diagonal entries are the same. A Hankel matrix corresponding to a vector $y = [y_1, y_2, \dots, y_7]$ is as follows:

$$\begin{bmatrix} y_1 & y_2 & y_3 & y_4 & y_5 \\ y_2 & y_3 & y_4 & y_5 & y_6 \\ y_3 & y_4 & y_5 & y_6 & y_7 \end{bmatrix}.$$

Given the observation of noisy system output, the goal in stochastic system realization (SSR) problem is to find a minimal order autoregressive moving-average model (Fazel et al., 2013; Yu et al., 2014). The order of such a model is equal to the rank of the Hankel matrix consisting of the exact process covariances. Hence, finding a low-order model is equivalent to learning a low-rank Hankel matrix close to the given data y (Fazel et al., 2013; Markovsky & Usevich, 2013; Markovsky, 2014).

The function $g(\mathbf{U})$ specialized for the case of low-rank Hankel matrix learning with square loss is as follows:

$$g(\mathbf{U}) = \max_{s_t \in \mathbb{R}^d \forall t, z \in \mathbb{R}^{d+T-1}} z^\top y - \frac{\|z\|^2}{4C} - \frac{1}{2} \sum_{t=1}^T \|\mathbf{U}^\top s_t\|^2$$

subject to : $\sum_{\substack{(i,t): i+t=k, \\ 1 \leq i \leq d, 1 \leq t \leq T}} s_{ti} = z_k \quad \forall k = 2, \dots, d+T.$

We solve the above problem via a preconditioned conjugate gradients (PCG) algorithm (Barrett et al., 1994). The equality constraints are handled efficiently by using an affine projection operator. Since dT constraints need to be satisfied, the computational cost of computing $g(\mathbf{U})$ is $O(dTkr)$, where k is the number of iterations of PCG. The overall per-iteration complexity of Algorithm 1 is $O(dTkr + dr + r^3)$.

5.5 Multi-task feature learning

Given several tasks, the aim in multi-task feature learning (MTFL) is to learn the model parameter w_t for each task t such that they share a low-dimensional latent feature space. Argyriou et al. (2008) proposed to employ the squared trace-norm regularizer on the model parameter matrix $\mathbf{W} = [w_1, \dots, w_T]$ in the MTFL setting. Each task t has an input/output training data set $\{\mathbf{X}_t, y_t\}$, where $\mathbf{X}_t \in \mathbb{R}^{m \times d}$ and $y_t \in \mathbb{R}^m$. The square loss function for MTFL can be expressed as $L(\mathbf{W}, \mathbf{Y}; \{\mathbf{X}_1, \dots, \mathbf{X}_T\}) = \sum_{t=1}^T \|y_t - \mathbf{X}_t w_t\|^2$. The proposed generic formulation for structured low-rank matrix learning (5) can easily be specialized to MTFL setting, with the function $g(\mathbf{U})$ being as follows:

$$g(\mathbf{U}) = \sum_{t=1}^T \max_{z_t \in \mathbb{R}^{m_t}} \langle y_t, z_t \rangle - \frac{\|z_t\|^2}{4C} - \frac{\|\mathbf{U}^\top \mathbf{X}_t^\top z_t\|^2}{2}.$$

In this case, $g(\mathbf{U})$ can be computed in closed form and costs $O(T(mr^2 + r^3 + mrd))$. Hence, the per-iteration complexity of Algorithm 1 for MTFL is $O(T(mr^2 + r^3 + mrd) + dr + r^3)$.

6 Experiments

In this section, we evaluate the generalization performance as well as computational efficiency of our approach against state-of-the-art in five different applications — matrix completion, robust matrix completion, non-negative matrix completion, Hankel matrix learning, and multi-task learning. It should be emphasized that state-of-the-art in each application are different and to the best of our knowledge there does not exist a unified framework for solving such applications. All our algorithms are implemented using the Manopt toolbox (Boumal et al., 2014). Implementation and parameter tuning details, data set statistics, and additional results are provided in the supplementary material.

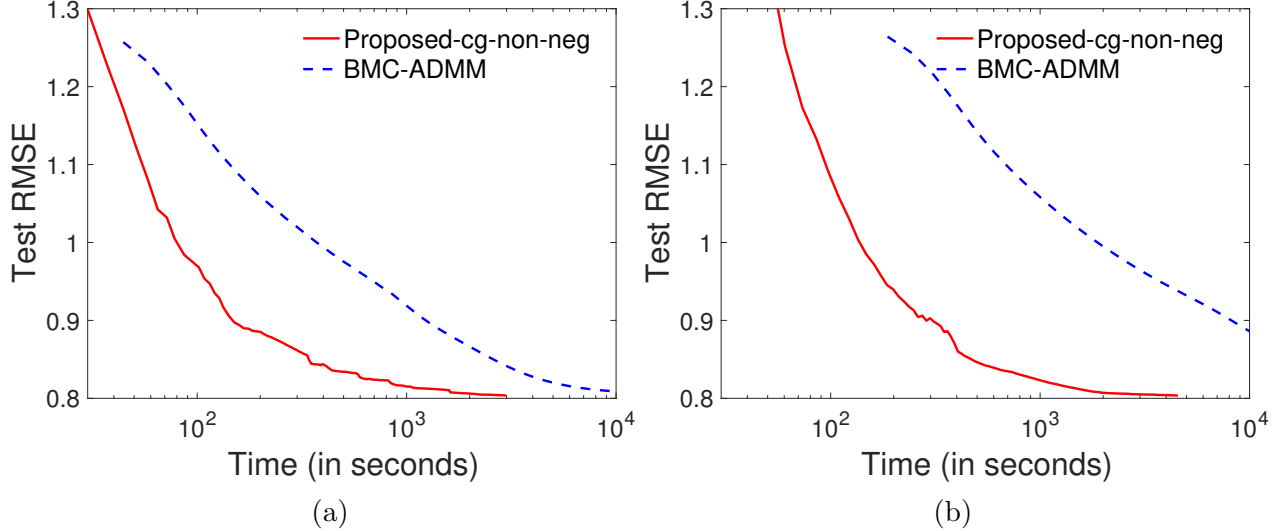


Figure 1: Evolution of test RMSE on non-negative matrix completion problem: (a) MovieLens10m data set, and (b) MovieLens20m data set. The proposed algorithm Proposed-cg-non-neg outperforms state-of-the-art BMC-ADMM solver by an order of magnitude in MovieLens20m.

Table 1: Mean test RMSE on non-negative matrix completion problems. Our algorithm, Proposed-cg-non-neg, obtains the best generalization performance. All entries have standard deviation of 0.001.

	ML10m	ML20m
Proposed-cg-non-neg	0.804	0.802
BMC-ADMM	0.809	0.852

Non-negative matrix completion

Baseline techniques and parameter settings: We compare our first-order non-negative matrix completion algorithm, Proposed-cg-non-neg, against state-of-the-art BMC-ADMM algorithm (Fang et al., 2017). BMC-ADMM has carefully designed update rules to ensure an efficient computational and space complexity. We experiment on two large-scale real world data sets: MovieLens10m (ML10m), and MovieLens20m (ML20m) (MovieLens, 1997). We run both the methods on ten random 80/20 train/test splits. The rank r for Proposed-cg-non-neg as well as the maximum rank for BMC-ADMM are set as 10. We cross-validate the regularization parameters for best performance of both algorithms.

Results: Figures 1(a)&(b) plot the evolution of the root mean squared error on the test set (test RMSE) against the training time for both algorithms on the two data sets. We observe that our algorithm Proposed-cg-non-neg is significantly faster than BMC-ADMM in converging to the best test RMSE. Table 1 reports the mean test RMSE obtained by each algorithm.

Hankel matrix learning

Baseline techniques and parameter settings: We perform a small-scale and a large-scale experiment for learning a low-rank Hankel matrix. We compare our first-order low-rank Hankel matrix learning algorithm, Proposed-cg-hk, with three state-of-the-art solvers: GCG (Yu et al.,

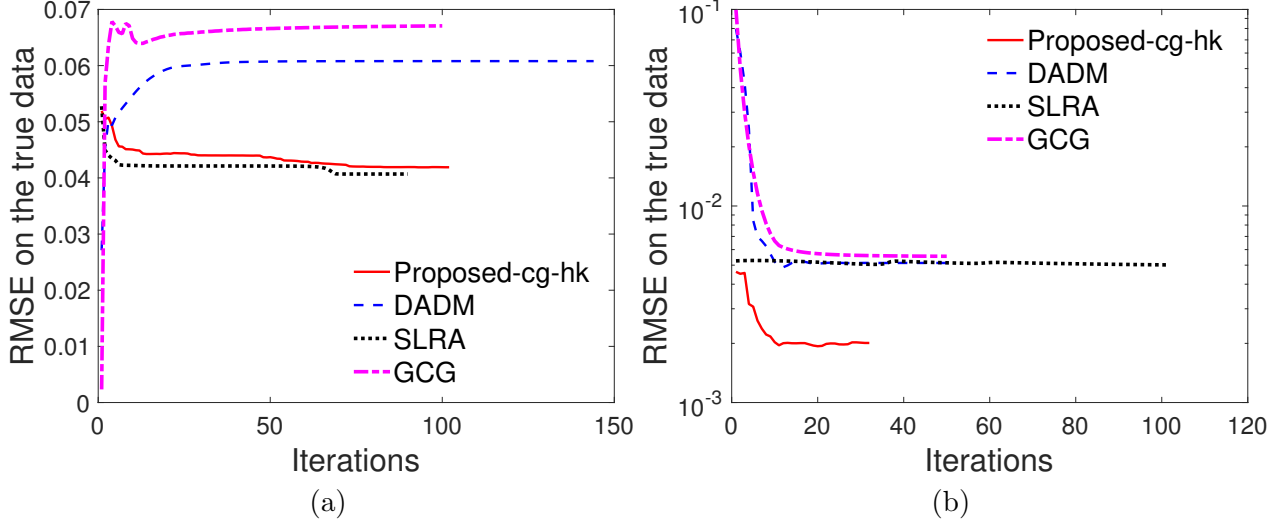


Figure 2: Performance on different stochastic system realization problems — learning low-rank Hankel matrices: (a) small-scale data set (Fazel et al., 2013; Yu et al., 2014), and (b) large-scale data set (Markovsky, 2014; Markovsky & Usevich, 2014).

2014), SLRA (Markovsky, 2014; Markovsky & Usevich, 2014), and DADM (Fazel et al., 2013). Since GCG and DADM have a nuclear norm regularizer, we tune the regularization parameter to vary the rank. Proposed-cg-hk is initialized with a random \mathbf{U} matrix, SLRA employ SVD based initialization provided by its authors, and GCG and DADM are initialized with the input training matrix. Both DADM and GCG are convex approaches and their converged solutions are independent of the initialization.

Results: In our first experiment, the data is generated in accordance with the setting detailed in (Fazel et al., 2013; Yu et al., 2014), with $d = 21$, $T = 100$, and $r = 10$. Figure 2(a) shows the variation of RMSE with respect to true data (true RMSE) across iterations. The training data is a noisy version of true data. We observe that our algorithm outperforms GCG and DADM and matches SLRA in terms of generalization performance. The true RMSE at convergence is: **0.041** (SLRA), 0.042 (Proposed-cg-hk), 0.061 (DADM), and 0.067 (GCG).

In our second experiment, we generate the data in accordance with the setting detailed in (Markovsky, 2014; Markovsky & Usevich, 2014). We set $d = 1000$, $T = 10000$, and $r = 5$ and repeat the above experiment. The true RMSE is plotted in Figure 2(b). We observe that our algorithm obtain significantly better true RMSE than GCG, DADM, and SLRA.

Matrix completion

Baseline techniques and parameter settings: Our first- and second-order matrix completion algorithms (Section 5.1 and Algorithm 1) with square loss are denoted by Proposed-cg-sq and Proposed-tr-sq, respectively. We compare against state-of-the-art fixed-rank and nuclear norm minimization based matrix completion solvers: APGL: accelerated proximal gradient algorithm for nuclear norm minimization (Toh & Yun, 2010), Active ALT: first-order nuclear norm solver based on active subspace selection (Hsieh & Olsen, 2014), R3MC: fixed-rank Riemannian preconditioned nonlinear conjugate gradient algorithm (Mishra & Sepulchre, 2014), LMaFit: nonlinear successive over-relaxation algorithm based on alternate least squares (Wen et al., 2012), MMBS: fixed-rank second-order nuclear norm minimization algorithm (Mishra et al., 2013), RTRMC: fixed-rank second-order

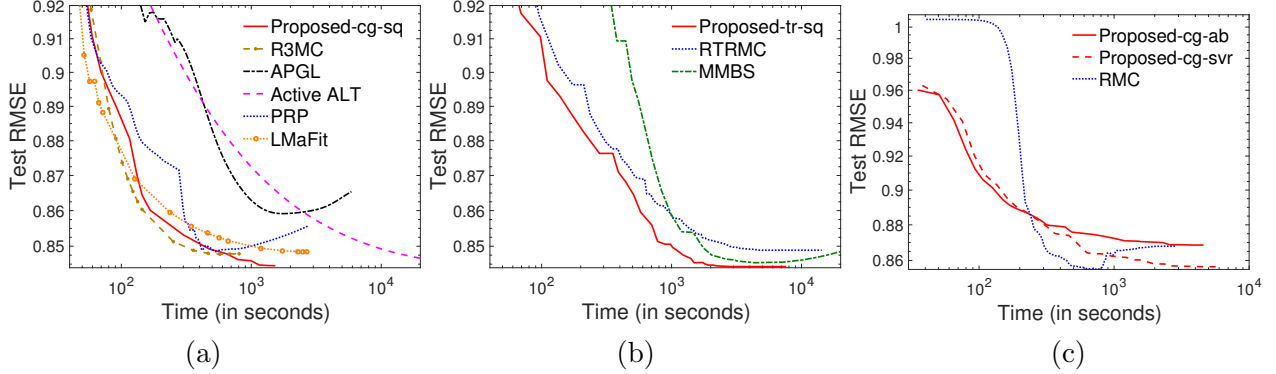


Figure 3: Evolution of test RMSE on the Netflix data set. (a)&(b) Comparison of first- and second-order matrix completion algorithms, respectively; (c) Comparison of robust matrix completion algorithms. In both standard and robust matrix completion settings, our algorithms converge to the best generalization performance.

Riemannian preconditioned algorithm on the Grassmann manifold (Boumal & Absil, 2011, 2015), and PRP: a recent proximal Riemannian pursuit algorithm (Tan et al., 2016).

The regularization parameters for respective algorithms are cross-validated to obtain their best performance. The initialization for all the algorithms is based on the first few singular vectors of the given partially complete matrix \mathbf{Y} (Boumal & Absil, 2015). All the fixed algorithms (R3MC, LMaFit, MMBS, RTRMC, Proposed-cg-sq, Proposed-tr-sq) are provided the rank $r = 10$. In all variable rank approaches (APGL, Active ALT, PRP), the maximum rank parameter is set to 10. We run all the methods on ten random 80/20 train/test splits.

Results: Figures 3(a)&(b) display the evolution of test RMSE against the training time on the Netflix data set (Recht & Ré, 2013) for first- and second-order algorithms, respectively. Proposed-cg-sq is among the most efficient first-order method and Proposed-tr-sq is the best second-order method. Both our algorithms attain the lowest test RMSE: 0.845 (Proposed-cg-sq) and 0.844 (Proposed-tr-sq).

Robust matrix completion

Baseline techniques and parameter settings: We compare our robust matrix learning algorithms (Section 5.2 and Algorithm 1) against RMC (Cambier & Absil, 2016), a state-of-the-art first-order Riemannian optimization algorithm employing approximate ℓ_1 -loss (via successive smooth pseudo-Huber loss). We develop two robust matrix completion algorithms within our framework: Proposed-cg-ab (our first-order algorithm with ℓ_1 -loss), and Proposed-cg-svr (our first-order algorithm employing ϵ -SVR loss). It should be emphasized that the non-smooth nature of ℓ_1 -loss and ϵ -SVR loss makes them challenging to optimize in large-scale low-rank setting. We follow the same experimental setup as described for the case of matrix completion.

Results: Figure 3(c) shows the results on the Netflix data set. We observe that both our algorithms scale effortlessly on the Netflix data set, with Proposed-cg-svr obtaining the best generalization result. It should be noted that RMC approximates ℓ_1 -loss only towards the end of its iterations. The test RMSE obtained at convergence are: **0.857** (Proposed-cg-svr), 0.869 (Proposed-cg-ab), and 0.868 (RMC).

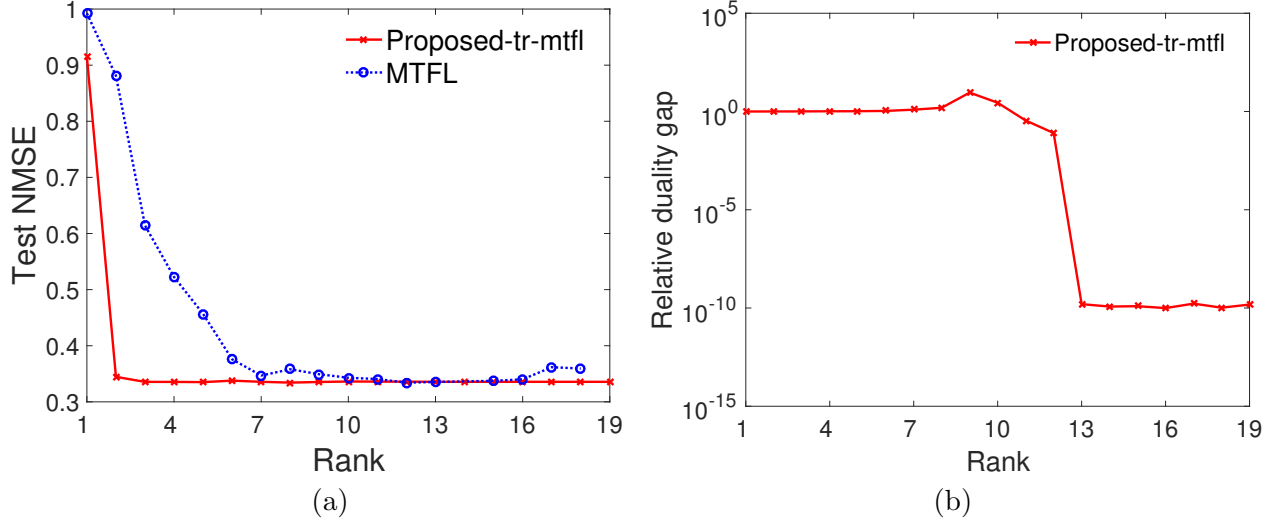


Figure 4: Multi-task feature learning problem: (a) Generalization performance vs rank. Our algorithm, Proposed-tr-mtfl, obtains better generalization performance than MTFL (Argyriou et al., 2008); (b) Relative duality gap vs rank for our algorithm.

Multi-task learning

Baseline techniques and parameter settings: We compare the generalization performance of our multi-task feature learning algorithm Proposed-tr-mtfl (Section 5.5 and Algorithm 1) with the convex multi-task feature learning algorithm MTFL (Argyriou et al., 2008). Optimal solution for MTFL at different ranks is obtained by tracing the solution path with respect to the regularization parameter, whose value is varied as $\{2^{-8}, 2^{-7}, \dots, 2^{24}\}$. We vary the rank parameter r in our algorithm to obtain different ranked solutions for a given C . The experiments are performed on two benchmark multi-task regression data sets: a) Parkinsons: we need to predict the Parkinson’s disease symptom score of 42 patients (Frank & Asuncion, 2010); b) School: we need to predict performance of all students in 139 schools (Argyriou et al., 2008). Following existing works (Argyriou et al., 2008; Zhang & Yeung, 2010), we report the normalized mean square error over the test set (test NMSE).

Results: Figure 4(a) present the results on the Parkinsons data set. We observe from the figure that our method achieves the better generalization performance at low ranks compared to MTFL. Figure 4(b) plots the variation of duality gap with rank for our algorithm. We observe that as the rank is varied from low to high, we converge to the globally optimal solution of (4) and obtain the duality gap close to zero. Similar results are obtained on the School data set.

7 Conclusion

We have proposed a novel factorization for structured low-rank matrix learning problems, which stems from the application of duality theory and rank-constrained parameterization of positive semi-definite matrices. This allows to develop a conceptually simpler and unified optimization framework for various applications. State-of-the-art performance of our algorithms on several applications demonstrate the efficacy of our approach.

Acknowledgement

We thank Léopold Cambier, Ivan Markovsky, and Konstantin Usevich for useful discussions on the work. We thank Adams Wei Yu and Mingkui Tan for making their codes available.

References

- Absil, P.-A., Mahony, R., and Sepulchre, R. *Optimization Algorithms on Matrix Manifolds*. Princeton University Press, Princeton, NJ, 2008.
- Amit, Y., Fink, M., Srebro, N., and Ullman, S. Uncovering shared structures in multiclass classification. In *International Conference on Machine Learning (ICML)*, pp. 17–24, 2007.
- Argyriou, A., Evgeniou, T., and Pontil, M. Multi-task feature learning. In *Neural Information Processing Systems conference (NIPS)*, 2006.
- Argyriou, A., Evgeniou, T., and Pontil, M. Convex multi-task feature learning. *Machine Learning*, 73:243–272, 2008.
- Barrett, R., Berry, M., Chan, T. F., Demmel, J., Donato, J., Dongarra, J., Eijkhout, V., Pozo, R., Romine, C., and der Vorst, H. Van. *Templates for the Solution of Linear Systems: Building Blocks for Iterative Methods, 2nd Edition*. SIAM, 1994.
- Bertsekas, D. *Nonlinear Programming*. Athena Scientific, 1999. URL <http://www.athenasc.com/nonlinbook.html>.
- Bhaskar, S. A. and Javanmard, A. 1-bit matrix completion under exact low-rank constraint. In *Annual Conference on Information Sciences and Systems (CISS)*, pp. 1–6, 2015.
- Bonnans, J. F. and Shapiro, A. *Perturbation Analysis of Optimization Problems*. Springer-Verlag, 2000.
- Boumal, N. and Absil, P.-A. RTRMC: A Riemannian trust-region method for low-rank matrix completion. In *Advances in Neural Information Processing Systems 24 (NIPS)*, pp. 406–414, 2011.
- Boumal, N. and Absil, P.-A. Low-rank matrix completion via preconditioned optimization on the Grassmann manifold. *Linear Algebra and its Applications*, 475:200–239, 2015.
- Boumal, N., Mishra, B., Absil, P.-A., and Sepulchre, R. Manopt: a Matlab toolbox for optimization on manifolds. *Journal of Machine Learning Research*, 15(Apr):1455–1459, 2014.
- Box, G. E. P. and Jenkins, G. *Time Series Analysis, Forecasting and Control*. Holden-Day, Incorporated, 1990.
- Boyd, S. and Vandenberghe, L. *Convex Optimization*. Cambridge University Press, 2004. URL <http://www.stanford.edu/~boyd/cvxbook/>.
- Cai, J. F., Candès, E. J., and Shen, Z. A singular value thresholding algorithm for matrix completion. *SIAM Journal on Optimization*, 20(4):1956–1982, 2010.
- Cambier, L. and Absil, P. A. Robust low-rank matrix completion by Riemannian optimization. *SIAM J. Sci. Comput.*, 38(5):S440–S460, 2016.

- Candès, E. J. and Plan, Y. Matrix completion with noise. *Proceedings of the IEEE*, 98(6):925–936, 2009.
- Candès, E. J. and Recht, B. Exact matrix completion via convex optimization. *Foundations of Computational Mathematics*, 9(6):717–772, 2009.
- Candès, E. J., Li, X., Ma, Y., and Wright, J. Robust principal component analysis? *Journal of the ACM (JACM)*, 58(3):11, 2011.
- Ciliberto, C., Mroueh, Y., Poggio, T., and Rosasco, L. Convex learning of multiple tasks and their structure. In *International Conference on Machine learning (ICML)*, 2015.
- Davenport, M. A., Plan, Y., van den Berg, E., and Wooters, M. 1-bit matrix completion. *Information and Inference*, 3(3):189–223, 2014.
- Edelman, A., Arias, T.A., and Smith, S.T. The geometry of algorithms with orthogonality constraints. *SIAM Journal on Matrix Analysis and Applications*, 20(2):303–353, 1998.
- Fang, H., Zhen, Z., Shao, Y., and Hsieh, C.-J. Improved bounded matrix completion for large-scale recommender systems. In *International Joint Conference on Artificial Intelligence (IJCAI)*, pp. 1654–1660, 2017.
- Fazel, M., Kei, P. T., Sun, D., and Tseng, P. Hankel matrix rank minimization with applications to system identification and realization. *SIAM Journal on Matrix Analysis and Applications*, 34(3):946–977, 2013.
- Frank, A. and Asuncion, A. UCI machine learning repository, 2010. URL <http://archive.ics.uci.edu/ml>.
- He, J., Balzano, L., and Szlam, A. Incremental gradient on the Grassmannian for online foreground and background separation in subsampled video. In *IEEE Conference on Computer Vision and Pattern Recognition (CVPR)*, pp. 1568–1575, 2012.
- Ho, C. H. and Lin, C. J. Large-scale linear support vector regression. *Journal of Machine Learning Research*, 13(1):3323–3348, 2012.
- Hsieh, C.-J. and Olsen, P. A. Nuclear norm minimization via active subspace selection. In *International Conference on Machine learning (ICML)*, 2014.
- Ji, S. and Ye, J. An accelerated gradient method for trace norm minimization. In *International Conference on Machine Learning (ICML)*, 2009.
- Journée, M., Bach, F., Absil, P.-A., and Sepulchre, R. Low-rank optimization on the cone of positive semidefinite matrices. *SIAM Journal on Optimization*, 20(5):2327–2351, 2010.
- Kannan, R., Ishteva, M., and Park, H. Bounded matrix low rank approximation. In *IEEE International Conference on Data Mining (ICDM)*, 2012.
- Kim, D., Sra, S., and Dhillon, I. S. A non-monotonic method for large-scale non-negative least squares. *Optimization Methods and Software*, 28(5):1012–1039, 2013.
- Marecek, J., Richtarik, P., and Takac, M. Matrix completion under interval uncertainty. *European Journal of Operational Research*, 256(1):35–43, 2017.

- Markovsky, I. Recent progress on variable projection methods for structured low-rank approximation. *Signal Processing*, 96(Part B):406–419, 2014.
- Markovsky, I. and Usevich, K. Structured low-rank approximation with missing data. *SIAM Journal on Matrix Analysis and Applications*, 34(2):814–830, 2013.
- Markovsky, I. and Usevich, K. Software for weighted structured low-rank approximation. *J. Comput. Appl. Math.*, 256:278–292, 2014.
- Mishra, B. and Sepulchre, R. R3MC: A Riemannian three-factor algorithm for low-rank matrix completion. In *Proceedings of the 53rd IEEE Conference on Decision and Control (CDC)*, pp. 1137–1142, 2014.
- Mishra, B., Meyer, G., Bach, F., and Sepulchre, R. Low-rank optimization with trace norm penalty. *SIAM Journal on Optimization*, 23(4):2124–2149, 2013.
- MovieLens. MovieLens, 1997. URL <http://grouplens.org/datasets/movielens/>.
- Recht, B. and Ré, C. Parallel stochastic gradient algorithms for large-scale matrix completion. *Mathematical Programming Computation*, 5(2):201–226, 2013.
- Sato, H. and Iwai, T. A new, globally convergent Riemannian conjugate gradient method. *Optimization: A Journal of Mathematical Programming and Operations Research*, 64(4):1011–1031, 2013.
- Sato, H., Kasai, H., and Mishra, B. Riemannian stochastic variance reduced gradient. Technical report, arXiv preprint arXiv:1702.05594, 2017.
- Sion, M. On General Minimax Theorem. *Pacific Journal of Mathematics*, 1958.
- Sun, D. L. and Mazumder, R. Non-negative matrix completion for bandwidth extension: A convex optimization approach. In *IEEE International Workshop on Machine Learning for Signal Processing (MLSP)*, 2013.
- Tan, M., Xiao, S., Gao, J., Xu, D., van den Hengel, A., and Shi, Q. Proximal riemannian pursuit for large-scale trace-norm minimization. In *The IEEE Conference on Computer Vision and Pattern Recognition (CVPR)*, 2016.
- Toh, K. C. and Yun, S. An accelerated proximal gradient algorithm for nuclear norm regularized least squares problems. *Pacific Journal of Optimization*, 6(3):615–640, 2010.
- Tsagkatakis, G., Geelen, B., Jayapala, M., and Tsakalides, P. Non-negative matrix completion for the enhancement of snapshot mosaic multispectral imagery. In *IS&T International Symposium on Electronic Imaging, Image Sensors and Imaging Systems*, 2016.
- Vandereycken, B. Low-rank matrix completion by Riemannian optimization. *SIAM Journal on Optimization*, 23(2):1214–1236, 2013.
- Wen, Z., Yin, W., and Zhang, Y. Solving a low-rank factorization model for matrix completion by a nonlinear successive over-relaxation algorithm. *Mathematical Programming Computation*, 4(4):333–361, 2012.

- Wright, J., Ganesh, A., Rao, S., Peng, Y., and Ma, Y. Robust principal component analysis: Exact recovery of corrupted low-rank matrices via convex optimization. In *Neural Information Processing Systems conference (NIPS)*, 2009.
- Yan, M., Yang, Y., and Osher, S. Exact low-rank matrix completion from sparsely corrupted entries via adaptive outlier pursuit. *Journal of Scientific Computing*, 56(3):433–449, 2013.
- Yu, A. W., W., Ma, Y., Yu, G., Carbonell J., and S., Sra. Efficient structured matrix rank minimization. In *Advances in Neural Information Processing Systems (NIPS)*, 2014.
- Yuan, M., Ekici, A., Lu, Z., and Monteiro, R.D.C. Dimension reduction and coefficient estimation in multivariate linear regression. *Journal of the Royal Statistical Society: Series B (Statistical Methodology)*, 69(3):329–346, 2007.
- Zhang, H., Reddi, S. J., and Sra, S. Riemannian svrg: Fast stochastic optimization on Riemannian manifolds. In *Advances in Neural Information Processing Systems (NIPS)*, pp. 4592–4600, 2016.
- Zhang, Y. and Yeung, D. Y. A convex formulation for learning task relationships in multi-task learning. In *Uncertainty in Artificial Intelligence*, 2010.

Supplementary material

Abstract

Section A.1 contains the proof of Lemma 2 proposed in the main paper. Section A.2 contains the proof of Lemma 3 proposed in the main paper. Section A.3 contains the proof of Proposition 1 proposed in the main paper. Section A.4 briefly describes the Riemannian optimization framework employed in our algorithms discussed in Section 3 of the main paper. Section A.5 presents the complete experimental results and related details. The sections, equations, tables, figures and algorithms from the main paper are referred in their original numbers. The sections, equations, tables and figures introduced in this supplementary have the numbering scheme of the form ‘A.x’.

A.1 Lemma 2 and its Proof

Lemma 2 gives the dual problem of the following primal problem with respect to variable \mathbf{W} :

$$\min_{\Theta \in \mathcal{P}^d} \sum_{t=1}^T \min_{w_t \in \mathbb{R}^d} \frac{1}{2} w_t^\top \Theta^\dagger w_t + C \sum_{i=1}^d l(y_{ti}, w_{ti}) \quad (\text{A.1})$$

subject to $w_t \in \text{range}(\Theta), \forall t = 1, \dots, T$ and $\mathcal{A}(\mathbf{W}) = \mathbf{0}$, where $\text{range}(\Theta) = \{\Theta z : z \in \mathbb{R}^d\}$. In the following, we restate Lemma 2 from the main paper (for convenience) and prove it.

Lemma 2. *Let l_{ti}^* be the Fenchel conjugate function of the loss: $l_{ti} : \mathbb{R} \rightarrow \mathbb{R}, v \mapsto l(y_{ti}, v)$. The dual of (A.1) with respect to \mathbf{W} is*

$$\min_{\Theta \in \mathcal{P}^d} g(\Theta), \quad (\text{A.2})$$

where $g : \mathcal{P}^d \rightarrow \mathbb{R} : \Theta \mapsto g(\Theta)$ is the following convex function

$$g(\Theta) := \max_{s \in \mathbb{R}^n} \sum_{t=1}^T \left(\max_{z_t \in \mathbb{R}^d} -C \sum_{i=1}^d l_{ti}^* \left(\frac{-z_{ti}}{C} \right) - \frac{1}{2} (z_t + a_t)^\top \Theta (z_t + a_t) \right). \quad (\text{A.3})$$

Here, $a_t \in \mathbb{R}^d$ for $t = \{1, \dots, T\}$, where $[a_1, \dots, a_T] = \mathcal{A}^*(s)$ and $\mathcal{A}^* : \mathbb{R}^n \rightarrow \mathbb{R}^{d \times T}$ is the adjoint of \mathcal{A} . Furthermore, if Θ^* be the optimal solution of (A.2) and $\{s^*, (z_t^*)_{t=1}^T\}$ be the corresponding optimal solution of (A.3), then the optimal solution $\mathbf{W}^* := [w_1^*, \dots, w_T^*]$ of (A.1) is given by $w_t^* = \Theta^*(z_t^* + a_t^*)$, where $[a_1^*, \dots, a_T^*] = \mathcal{A}^*(s^*)$.

Proof. We derive the Fenchel dual function of $p : \mathbb{R}^{d \times T} \rightarrow \mathbb{R}$,

$$p(\mathbf{W}) = \sum_{t=1}^T \frac{1}{2} w_t^\top \Theta^\dagger w_t + C \sum_{i=1}^d l(y_{ti}, w_{ti}) \quad (\text{A.4})$$

subject to $w_t \in \text{range}(\Theta), \forall t = 1, \dots, T$ and $\mathcal{A}(\mathbf{W}) = \mathbf{0}$, where $\text{range}(\Theta) = \{\Theta z : z \in \mathbb{R}^d\}$. For this purpose, we introduce the auxiliary variables $u_t \in \mathbb{R}^d, \forall t = 1, \dots, T$ which satisfy the constraint $u_{ti} = w_{ti}$. We now introduce the dual variable $z = \{z_1, \dots, z_T\}$, $z_t \in \mathbb{R}^d$ corresponding to the

constraints $u_{ti} = w_{ti}$, and the dual variable $s \in \mathbb{R}^n$ corresponding to the constraint $\mathcal{A}(\mathbf{W}) = \mathbf{0}$. Then the Lagrangian L of (A.4) is given as:

$$L(\mathbf{W}, u, z, s) = \sum_{t=1}^T \left(\frac{1}{2} w_t^\top \Theta^\dagger w_t + C \sum_{i=1}^d l(y_{ti}, u_{ti}) + \sum_{i=1}^d z_{ti}(u_{ti} - w_{ti}) + i_{\text{range}(\Theta)}(w_t) \right) - \langle s, \mathcal{A}(\mathbf{W}) \rangle. \quad (\text{A.5})$$

where i_H is the indicator function for set H . The dual function q of p is defined as

$$q(z, s) = \min_{\mathbf{W} \in \mathbb{R}^{d \times T}, u_t \in \mathbb{R}^d \forall t} L(\mathbf{W}, u, z, s) \quad (\text{A.6})$$

Using the definition of the conjugate function (Boyd & Vandenberghe, 2004), we get

$$\begin{aligned} \min_{u_t \in \mathbb{R}^d} C \sum_{i=1}^d l(y_{ti}, u_{ti}) + \sum_{i=1}^d z_{ti} u_{ti} &= -C \sum_{i=1}^d \max_{u_{ti} \in \mathbb{R}} \left(\left(-\frac{z_{ti}}{C} \right) u_{ti} - l(y_{ti}, u_{ti}) \right) \\ &= -C \sum_{i=1}^d l_{ti}^* \left(\frac{-z_{ti}}{C} \right), \end{aligned} \quad (\text{A.7})$$

where l_{ti}^* be the Fenchel conjugate function of the loss: $l_{ti} : \mathbb{R} \rightarrow \mathbb{R}$, $v \mapsto l(y_{ti}, v)$.

We next compute the minimizer of L with respect to w_t . From the definition of the adjoint operator, it follows that

$$\langle s, \mathcal{A}(\mathbf{W}) \rangle = \langle \mathcal{A}^*(s), \mathbf{W} \rangle$$

We define $[a_1, \dots, a_T] = \mathcal{A}^*(s)$. Then the Lagrangian L can be re-written as

$$\begin{aligned} L(\mathbf{W}, u, z, s) &= \left(\sum_{t=1}^T \sum_{i=1}^d C l(y_{ti}, u_{ti}) + z_{ti} u_{ti} \right) \\ &+ \sum_{t=1}^T \left(-a_t^\top w_t + \frac{1}{2} w_t^\top \Theta^\dagger w_t + i_{\text{range}(\Theta)}(w_t) - \sum_{i=1}^d z_{ti} w_{ti} \right). \end{aligned}$$

The minimizer of L with respect to w_t satisfy the following conditions

$$\frac{\partial}{\partial w_t} \left(-a_t^\top w_t + \frac{1}{2} w_t^\top \Theta^\dagger w_t - \sum_{i=1}^d z_{ti} w_{ti} \right) = 0, \text{ and} \quad (\text{A.8})$$

$$w_t \in \text{range}(\Theta) \quad (\text{A.9})$$

which implies,

$$\Theta^\dagger w_t = z_t + a_t, \text{ subject to } w_t \in \text{range}(\Theta) \quad (\text{A.10})$$

Thus, the expression of the minimizer of L with respect to w_t is

$$w_t = \Theta(z_t + a_t).$$

Plugging the above result and (A.7) in the dual function (A.6), we obtain

$$q(z, s) = \sum_{t=1}^T \left(-C \sum_{i=1}^d l_{ti}^* \left(\frac{-z_{ti}}{C} \right) - \frac{1}{2} (z_t + a_t)^\top \Theta (z_t + a_t) \right)$$

□

A.2 Proof of Lemma 3

The gradient is computed by employing the Danskin's theorem (Bertsekas, 1999; Bonnans & Shapiro, 2000). The directional derivative of the gradient follows directly from the chain rule.

A.3 Proof of Proposition 1

For convenience, we are reproducing the Proposition 1 from the main paper. Our proposed formulation is

$$\min_{\mathbf{U} \in \mathbb{R}^{d \times r}, \|\mathbf{U}\|_F = 1} g(\mathbf{U}\mathbf{U}^\top), \quad (\text{A.11})$$

where the function $g(\mathbf{U}\mathbf{U}^\top)$ is defined as follows, *i.e.*,

$$g(\mathbf{U}\mathbf{U}^\top) := \max_{s \in \mathbb{R}^n} \sum_{t=1}^T \max_{z_t \in \mathbb{R}^d} \left(-C \sum_{i=1}^d l_{ti}^* \left(\frac{-z_{ti}}{C} \right) - \frac{1}{2} \left\| \mathbf{U}^\top (z_t + a_t) \right\|_F^2 \right). \quad (\text{A.12})$$

Proposition 1. *Let $\hat{\mathbf{U}}$ be a feasible solution of (A.11). Then, a candidate solution for (A.2) is $\hat{\Theta} = \hat{\mathbf{U}}\hat{\mathbf{U}}^\top$. Let $\{\hat{s}, (\hat{z}_t)_{t=1}^T\}$ be the optimal solution of the convex problem in (A.12) at $\hat{\mathbf{U}}$. In addition, let σ_1 be the maximum singular of the matrix whose t^{th} column is $(\hat{z}_t + \hat{a}_t)$, where $[\hat{a}_1, \dots, \hat{a}_T] = \mathcal{A}^*(\hat{s})$. The duality gap (Δ) associated with $\{\hat{\Theta}, \hat{s}, (\hat{z}_t)_{t=1}^T\}$ for (A.2) is given by*

$$\Delta = \frac{1}{2} \left(\sigma_1^2 - \sum_{t=1}^T \left\| \hat{\mathbf{U}}^\top (\hat{z}_t + \hat{a}_t) \right\|^2 \right). \quad (\text{A.13})$$

Proof. Given $\hat{\Theta} = \hat{\mathbf{U}}\hat{\mathbf{U}}^\top$ as described above, the objective value of the min-max problem (A.2) is

$$g(\hat{\Theta}) = -C \sum_{t=1}^T \sum_{i=1}^d l_{ti}^* \left(\frac{-\hat{z}_{ti}}{C} \right) - \frac{1}{2} \sum_{t=1}^T \left\langle \hat{\Theta}, (\hat{z}_t + \hat{a}_t)(\hat{z}_t + \hat{a}_t)^\top \right\rangle. \quad (\text{A.14})$$

Using the min-max interchange (Sion, 1958), the max-min problem corresponding to (A.2) is as follows

$$\max_{s \in \mathbb{R}^n} \max_{z_t \in \mathbb{R}^d \forall t} \left(-C \sum_{t=1}^T \sum_{i=1}^d l_{ti}^* \left(\frac{-z_{ti}}{C} \right) - \frac{1}{2} B \right) \quad (\text{A.15})$$

where

$$B = \max_{\Theta \in \mathcal{P}^d} \left\langle \hat{\Theta}, \sum_{t=1}^T (\hat{z}_t + \hat{a}_t)(\hat{z}_t + \hat{a}_t)^\top \right\rangle. \quad (\text{A.16})$$

Note that problem (A.16) is a well studied problem in the duality theory. It is one of the definitions of the spectral norm (maximum eigenvalue of a matrix) – as the dual of the trace norm (Boyd & Vandenberghe, 2004). Its optimal value is the spectral norm of the matrix $\sum_{t=1}^T (\hat{z}_t + \hat{a}_t)(\hat{z}_t + \hat{a}_t)^\top$ (Boyd & Vandenberghe, 2004). Let σ_1 be the maximum singular of the matrix $E = \sum_{t=1}^T (\hat{z}_t + \hat{a}_t)(\hat{z}_t + \hat{a}_t)^\top$. Then the spectral norm of E is σ_1^2 . Note that the t^{th} column of E is $(\hat{z}_t + \hat{a}_t)$. Putting together the above result, the objective value of the max-min problem, given $\{\hat{s}, (\hat{z}_t)_{t=1}^T\}$ is

$$G = -C \sum_{t=1}^T \sum_{i=1}^d l_{ti}^* \left(\frac{-\hat{z}_{ti}}{C} \right) - \frac{1}{2} \sigma_1^2.$$

Therefor, the duality gap (Δ) associated with $\{\hat{\Theta}, \hat{s}, (\hat{z}_t)_{t=1}^T\}$ for problem (A.2) is given by

$$\begin{aligned}\Delta &= g(\hat{\Theta}) - G \\ &= \frac{1}{2} \left(\sigma_1^2 - \sum_{t=1}^T \left\langle \hat{\Theta}, (\hat{z}_t + \hat{a}_t)(\hat{z}_t + \hat{a}_t)^\top \right\rangle \right) \\ &= \frac{1}{2} \left(\sigma_1^2 - \sum_{t=1}^T \left\| \hat{\mathbf{U}}^\top (\hat{z}_t + \hat{a}_t) \right\|^2 \right)\end{aligned}\tag{A.17}$$

The last equality is obtained by using $\hat{\Theta} = \hat{\mathbf{U}}\hat{\mathbf{U}}^\top$. \square

A.4 Optimization on Spectrahedron

We are interested in the optimization problem of the form

$$\min_{\Theta \in \mathcal{P}^d} f(\Theta), \tag{A.18}$$

where \mathcal{P}^d is the set of $d \times d$ positive semi-definite matrices with unit trace and $f : \mathcal{P}^d \rightarrow \mathbb{R}$ is a smooth function. A specific interest is when we seek matrices of rank r . Using the parameterization $\Theta = \mathbf{U}\mathbf{U}^\top$, the problem (A.18) is formulated as

$$\min_{\mathbf{U} \in \mathcal{S}_r^d} f(\mathbf{U}\mathbf{U}^\top), \tag{A.19}$$

where $\mathcal{S}_r^d := \{\mathbf{U} \in \mathbb{R}^{d \times r} : \|\mathbf{U}\|_F = 1\}$, which is called the spectrahedron manifold (Journée et al., 2010). It should be emphasized the objective function in (A.19) is *invariant* to the post multiplication of \mathbf{U} with orthogonal matrices of size $r \times r$, i.e., $\mathbf{U}\mathbf{U}^\top = \mathbf{U}\mathbf{Q}(\mathbf{U}\mathbf{Q})^\top$ for all $\mathbf{Q} \in \mathcal{O}(r)$, which is the set of orthogonal matrices of size $r \times r$ such that $\mathbf{Q}\mathbf{Q}^\top = \mathbf{Q}^\top\mathbf{Q} = \mathbf{I}$. An implication of the this observation is that the minimizers of (A.19) are no longer isolated in the matrix space, but are isolated in the quotient space, which is the set of equivalence classes $[\mathbf{U}] := \{\mathbf{U}\mathbf{Q} : \mathbf{Q}\mathbf{Q}^\top = \mathbf{Q}^\top\mathbf{Q} = \mathbf{I}\}$. Consequently, the search space is

$$\mathcal{M} := \mathcal{S}_r^d / \mathcal{O}(r). \tag{A.20}$$

In other words, the optimization problem (A.19) has the structure of optimization on the *quotient* manifold, i.e.,

$$\min_{[\mathbf{U}] \in \mathcal{M}} f([\mathbf{U}]), \tag{A.21}$$

but numerically, by necessity, algorithms are implemented in the matrix space \mathcal{S}_r^d , which is also called the *total space*.

Below, we briefly discuss the manifold ingredients and their matrix characterizations for (A.21). Specific details of the spectrahedron manifold are discussed in (Journée et al., 2010). A general introduction to manifold optimization and numerical algorithms on manifolds are discussed in (Absil et al., 2008).

A.4.1 Tangent vector representation as horizontal lifts

Since the manifold \mathcal{M} , defined in (A.20), is an abstract space, the elements of its tangent space $T_{[\mathbf{U}]} \mathcal{M}$ at $[\mathbf{U}]$ also call for a matrix representation in the tangent space $T_{\mathbf{U}} \mathcal{S}_r^d$ that respects the equivalence relation $\mathbf{U}\mathbf{U}^\top = \mathbf{U}\mathbf{Q}(\mathbf{U}\mathbf{Q})^\top$ for all $\mathbf{Q} \in \mathcal{O}(r)$. Equivalently, the matrix representation

Table A.1: Matrix characterization of notions on the quotient manifold $\mathcal{S}_r^d/\mathcal{O}(r)$.

Manifold notions	Matrix representations
Matrix representation of an element	\mathbf{U}
Total space \mathcal{S}_r^d	$\{\mathbf{U} \in \mathbb{R}^{d \times r} : \ \mathbf{U}\ _F = 1\}$
Group action	$\mathbf{U} \mapsto \mathbf{U}\mathbf{Q}$, where $\mathbf{Q} \in \mathcal{O}(r)$.
Quotient space \mathcal{M}	$\mathcal{S}_r^d/\mathcal{O}(r)$
Tangent vectors in the total space \mathcal{S}_r^d at \mathbf{U}	$\{\mathbf{Z} \in \mathbb{R}^{d \times r} : \text{trace}(\mathbf{Z}^\top \mathbf{U}) = 0\}$
Metric between the tangent vector $\xi_{\mathbf{U}}, \eta_{\mathbf{U}} \in T_{\mathbf{U}}\mathcal{S}_r^d$	$\text{trace}(\xi_{\mathbf{U}}^\top \eta_{\mathbf{U}})$
Vertical tangent vectors at \mathbf{U}	$\{\mathbf{U}\mathbf{\Lambda} : \mathbf{\Lambda} \in \mathbb{R}^{r \times r}, \mathbf{\Lambda}^\top = -\mathbf{\Lambda}\}$
Horizontal tangent vectors	$\{\xi_{\mathbf{U}} \in T_{\mathbf{U}}\mathcal{S}_r^d : \xi_{\mathbf{U}}^\top \mathbf{U} = \mathbf{U}^\top \xi_{\mathbf{U}}\}$

of $T_{[\mathbf{U}]} \mathcal{M}$ should be restricted to the directions in the tangent space $T_{\mathbf{U}}\mathcal{S}_r^d$ on the total space \mathcal{S}_r^d at \mathbf{U} that do not induce a displacement along the equivalence class $[\mathbf{U}]$. In particular, we decompose $T_{\mathbf{U}}\mathcal{S}_r^d$ into complementary subspaces, the *vertical* $\mathcal{V}_{\mathbf{U}}$ and *horizontal* $\mathcal{H}_{\mathbf{U}}$ subspaces, such that $\mathcal{V}_{\mathbf{U}} \oplus \mathcal{H}_{\mathbf{U}} = T_{\mathbf{U}}\mathcal{S}_r^d$.

The vertical space $\mathcal{V}_{\mathbf{U}}$ is the tangent space of the equivalence class $[\mathbf{U}]$. On the other hand, the horizontal space $\mathcal{H}_{\mathbf{U}}$, which is any complementary subspace to $\mathcal{V}_{\mathbf{U}}$ in $T_{\mathbf{U}}\mathcal{S}_r^d$, provides a valid matrix representation of the abstract tangent space $T_{[\mathbf{U}]} \mathcal{M}$. An abstract tangent vector $\xi_{[\mathbf{U}]} \in T_{[\mathbf{U}]} \mathcal{M}$ at $[\mathbf{U}]$ has a unique element in the horizontal space $\xi_{\mathbf{U}} \in \mathcal{H}_{\mathbf{U}}$ that is called its *horizontal lift*. Our specific choice of the horizontal space is the subspace of $T_{\mathbf{U}}\mathcal{S}_r^d$ that is the *orthogonal complement* of $\mathcal{V}_{\mathbf{U}}$ in the sense of a *Riemannian metric*.

The Riemannian metric at a point on the manifold is a inner product that is defined in the tangent space. An additional requirement is that the inner product needs to be *invariant* along the equivalence classes (Absil et al., 2008, Chapter 3). One particular choice of the Riemannian metric on the total space \mathcal{S}_r^d is

$$\langle \xi_{\mathbf{U}}, \eta_{\mathbf{U}} \rangle_{\mathbf{U}} := \text{trace}(\xi_{\mathbf{U}}^\top \eta_{\mathbf{U}}), \quad (\text{A.22})$$

where $\xi_{\mathbf{U}}, \eta_{\mathbf{U}} \in T_{\mathbf{U}}\mathcal{S}_r^d$. The choice of the metric (A.22) leads to a natural choice of the metric on the quotient manifold, i.e.,

$$\langle \xi_{[\mathbf{U}]}, \eta_{[\mathbf{U}]} \rangle_{[\mathbf{U}]} := \text{trace}(\xi_{\mathbf{U}}^\top \eta_{\mathbf{U}}), \quad (\text{A.23})$$

where $\xi_{[\mathbf{U}]}$ and $\eta_{[\mathbf{U}]}$ are abstract tangent vectors in $T_{[\mathbf{U}]} \mathcal{M}$ and $\xi_{\mathbf{U}}$ and $\eta_{\mathbf{U}}$ are their horizontal lifts in the total space \mathcal{S}_r^d , respectively. Endowed with this Riemannian metric, the quotient manifold \mathcal{M} is called a *Riemannian* quotient manifold of \mathcal{S}_r^d .

Table A.1 summarizes the concrete matrix operations involved in computing horizontal vectors.

Additionally, starting from an arbitrary matrix (an element in the ambient dimension $\mathbb{R}^{d \times r}$), two linear projections are needed: the first projection $\Psi_{\mathbf{U}}$ is onto the tangent space $T_{\mathbf{U}}\mathcal{S}_r^d$ of the total space, while the second projection $\Pi_{\mathbf{U}}$ is onto the horizontal subspace $\mathcal{H}_{\mathbf{U}}$.

Given a matrix $\mathbf{Z} \in \mathbb{R}^{d \times r}$, the projection operator $\Psi_{\mathbf{U}} : \mathbb{R}^{d \times r} \rightarrow T_{\mathbf{U}}\mathcal{S}_r^d : \mathbf{Z} \mapsto \Psi_{\mathbf{U}}(\mathbf{Z})$ on the tangent space is defined as

$$\Psi_{\mathbf{U}}(\mathbf{Z}) = \mathbf{Z} - \text{trace}(\mathbf{Z}^\top \mathbf{U})\mathbf{U}. \quad (\text{A.24})$$

Given a tangent vector $\xi_{\mathbf{U}} \in T_{\mathbf{U}}\mathcal{S}_r^d$, the projection operator $\Pi_{\mathbf{U}} : T_{\mathbf{U}}\mathcal{S}_r^d \rightarrow \mathcal{H}_{\mathbf{U}} : \xi_{\mathbf{U}} \mapsto \Pi_{\mathbf{U}}(\xi_{\mathbf{U}})$

on the horizontal space is defined as

$$\Pi_{\mathbf{U}}(\xi_{\mathbf{U}}) = \xi_{\mathbf{U}} - \mathbf{U}\mathbf{\Lambda}, \quad (\text{A.25})$$

where $\mathbf{\Lambda}$ is the solution to the *Lyapunov* equation

$$(\mathbf{U}^\top \mathbf{U})\mathbf{\Lambda} + \mathbf{\Lambda}(\mathbf{U}^\top \mathbf{U}) = \mathbf{U}^\top \xi_{\mathbf{U}} - \xi_{\mathbf{U}}^\top \mathbf{U}.$$

A.4.2 Retractions from Horizontal Space to Manifold

An iterative optimization algorithm involves computing a search direction (*e.g.*, the gradient direction) and then ?moving in that direction?. The default option on a Riemannian manifold is to move along geodesics, leading to the definition of the exponential map. Because the calculation of the exponential map can be computationally demanding, it is customary in the context of manifold optimization to relax the constraint of moving along geodesics. The exponential map is then relaxed to a *retraction* operation, which is any map $R_{\mathbf{U}} : \mathcal{H}_{\mathbf{U}} \rightarrow \mathcal{S}_r^d : \xi_{\mathbf{U}} \mapsto R_{\mathbf{U}}(\xi_{\mathbf{U}})$ that locally approximates the exponential map on the manifold (Absil et al., 2008, Definition 4.1.1). On the spectrahedron manifold, a natural retraction of choice is

$$R_{\mathbf{U}}(\xi_{\mathbf{U}}) := (\mathbf{U} + \xi_{\mathbf{U}}) / \|\mathbf{U} + \xi_{\mathbf{U}}\|_F, \quad (\text{A.26})$$

where $\|\cdot\|_F$ is the Frobenius norm and $\xi_{\mathbf{U}}$ is a search direction on the horizontal space $\mathcal{H}_{\mathbf{U}}$.

An update on the spectrahedron manifold is, thus, based on the update formula $\mathbf{U}_+ = R_{\mathbf{U}}(\xi_{\mathbf{U}})$.

A.4.3 Riemannian Gradient and Hessian Computations

The choice of the invariant metric (A.22) and the horizontal space turns the quotient manifold \mathcal{M} into a *Riemannian submersion* of $(\mathcal{S}_r^d, \langle \cdot, \cdot \rangle)$. As shown by (Absil et al., 2008), this special construction allows for a convenient matrix characterization of the gradient and the Hessian of a function on the abstract manifold \mathcal{M} .

The matrix characterization of the Riemannian gradient is

$$\text{grad}_{\mathbf{U}} f = \Psi_{\mathbf{U}}(\nabla_{\mathbf{U}} f), \quad (\text{A.27})$$

where $\nabla_{\mathbf{U}} f$ is the Euclidean gradient of the objective function f and $\Psi_{\mathbf{U}}$ is the tangent space projector (A.24).

An iterative algorithm that exploits second-order information usually requires the Hessian applied along a search direction. This is captured by the Riemannian Hessian operator Hess , whose matrix characterization, given a search direction $\xi_{\mathbf{U}} \in \mathcal{H}_{\mathbf{U}}$, is

$$\begin{aligned} \text{Hess}_{\mathbf{U}}[\xi_{\mathbf{U}}] = \Pi_{\mathbf{U}} \Big(& D\nabla f[\xi_{\mathbf{U}}] - \text{trace}((\nabla_{\mathbf{U}} f)^\top \mathbf{U}) \xi_{\mathbf{U}} \\ & - \text{trace}((\nabla_{\mathbf{U}} f)^\top \xi_{\mathbf{U}} + (D\nabla f[\xi_{\mathbf{U}}])^\top \mathbf{U}) \mathbf{U} \Big), \end{aligned} \quad (\text{A.28})$$

where $D\nabla f[\xi_{\mathbf{U}}]$ is the directional derivative of the Euclidean gradient $\nabla_{\mathbf{U}} f$ along $\xi_{\mathbf{U}}$ and $\Pi_{\mathbf{U}}$ is the horizontal space projector (A.25).

Finally, the formulas in (A.27) and (A.28) that the Riemannian gradient and Hessian operations require only the expressions of the standard (Euclidean) gradient of the objective function f and the directional derivative of this gradient (along a given search direction) to be supplied.

A.5 Experiments

In this section, we evaluate the generalization performance as well as computational efficiency of our approach against state-of-the-art in four different applications — matrix completion, robust matrix completion, Hankel matrix learning, and multi-task learning. All our algorithms are implemented using the Manopt toolbox (Boumal et al., 2014).

A.5.1 Matrix Completion

Our first- and second-order methods (Algorithm 1) with square loss are denoted by Proposed-cg-sq and Proposed-tr-sq, respectively.

Baseline techniques: We compare against state-of-the-art fixed-rank and nuclear norm minimization based matrix completion solvers:

- APGL: An accelerated proximal gradient approach for nuclear norm regularization with square loss function (Toh & Yun, 2010).
- Active ALT: State-of-the-art first-order nuclear norm solver based on active subspace selection (Hsieh & Olsen, 2014).
- MMBS: A second-order fixed rank nuclear norm minimization algorithm (Mishra et al., 2013). It employs an efficient factorization of the matrix \mathbf{W} which renders the trace norm regularizer differentiable in the primal formulation.
- R3MC: A non-linear conjugate gradient based approach for fixed rank matrix completion (Mishra & Sepulchre, 2014). It employs a Riemannian preconditioning technique, customized for the square loss function.
- RTRMC: It models fixed rank matrix completion problems with square loss on the Grassmann manifold and solves it via a second order preconditioned Riemannian trust-region method (Boumal & Absil, 2011, 2015).
- LMaFit: A nonlinear successive over-relaxation based approach for low rank matrix completion based on alternate least squares (Wen et al., 2012).
- PRP: a recent proximal Riemannian pursuit algorithm Tan et al. (2016).

Parameter settings: The regularization parameters for respective algorithms are cross-validated in the set $\{1e-6, 1e-5, \dots, 1e0\}$ to obtain their best generalization performance. The optimization strategies for the competing algorithm were set to those prescribed by their authors. For instance, line-search, continuation and truncation were kept on for APGL. The initialization for all the algorithms is based on the first few singular vectors of the given partially complete matrix \mathbf{Y} (Boumal & Absil, 2015). All the fixed algorithms (R3MC, LMaFit, MMBS, RTRMC, Proposed-cg-sq, Proposed-tr-sq) are provided the rank $r = 10$ for real data sets and $r = 5$ for synthetic data set. In all variable rank approaches (APGL, Active ALT, PRP), the maximum rank parameter is set to 10 for real data sets and 5 for synthetic data set. We run all the methods on ten random 80/20 train/test splits and report the average root mean squared error on the test set (test RMSE). We report the minimum test RMSE achieved after the algorithms have converged or have reached maximum number of iterations (maxIter). For first-order methods, maxIter is set to 500 for the Netflix data set and 200 for other smaller data sets. For second-order methods, maxIter is set to 100 for the Netflix data set and 60 for other smaller data sets.

Synthetic data set results. We choose $d = 5\,000$, $T = 500\,000$ and $r = 5$ to create a synthetic data set (with $< 1\%$ observed entries), following the procedure detailed by (Boumal & Absil, 2011, 2015). The number of observed entries for both training ($|\Omega|$) and testing was 15 149 850. The generalization performance of different methods is shown in Figure A.1(a). For the same run, we also plot the variation of the relative duality gap across iterations for our methods in figure A.1(b).

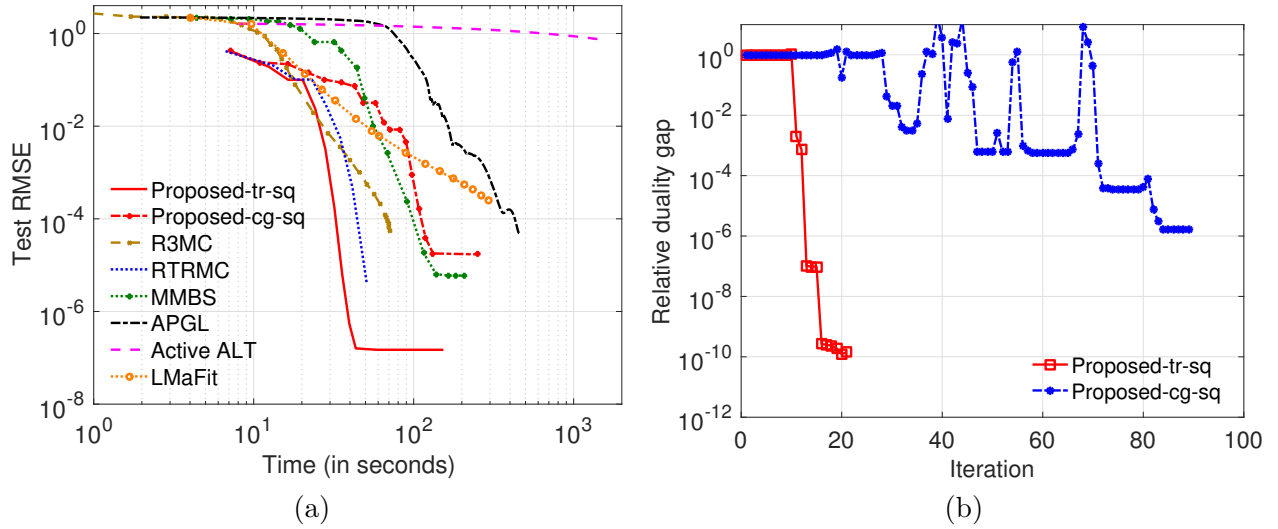


Figure A.1: (a) Evolution of test RMSE on the synthetic data set. Both our methods obtain very low test RMSE; (b) Variation of the relative duality gap per iteration for our methods on the synthetic data set. It can be observed that both our algorithms obtain very low relative duality gap.

Table A.2: Data set statistics for the matrix completion application.

	d	T	$ \Omega $
Netflix	17 770	480 189	100 198 805
ML10m	10 677	71 567	10 000 054
ML20m	26 744	138 493	20 000 263

Table A.3: Generalization performance of various algorithms on the matrix completion problem. The table reports mean test RMSE along with the standard deviation over ten random train-test split. The proposed algorithms achieve the lowest test RMSE.

	Netflix	MovieLens10m	MovieLens20m
Proposed	0.8443 ± 0.0001	0.8026 ± 0.0005	0.7962 ± 0.0003
Proposed-cg	0.8449 ± 0.0003	0.8026 ± 0.0005	0.7963 ± 0.0003
R3MC	0.8478 ± 0.0001	0.8070 ± 0.0004	0.7982 ± 0.0003
RTRMC	0.8489 ± 0.0001	0.8161 ± 0.0004	0.8044 ± 0.0005
APGL	0.8587 ± 0.0005	0.8283 ± 0.0009	0.8160 ± 0.0013
Active ALT	0.8463 ± 0.0005	0.8116 ± 0.0012	0.8033 ± 0.0008
MMBS	0.8454 ± 0.0002	0.8226 ± 0.0015	0.8053 ± 0.0008
LMaFit	0.8484 ± 0.0001	0.8082 ± 0.0005	0.7996 ± 0.0003
PRP	0.8488 ± 0.0007	0.8068 ± 0.0006	0.7987 ± 0.0008

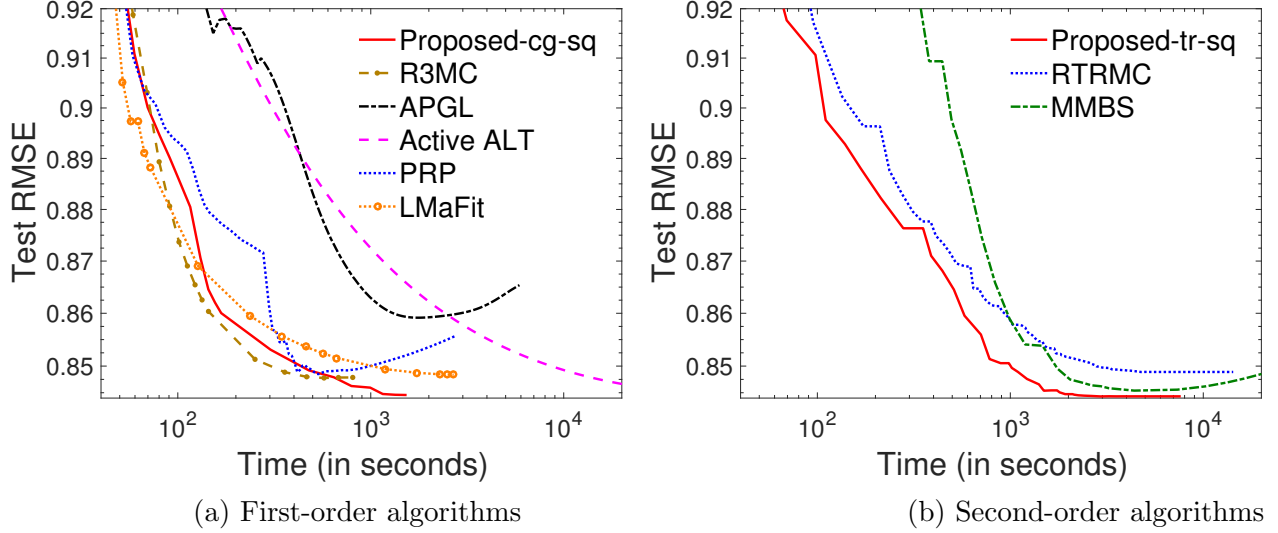


Figure A.2: Evolution of test RMSE on the Netflix data set

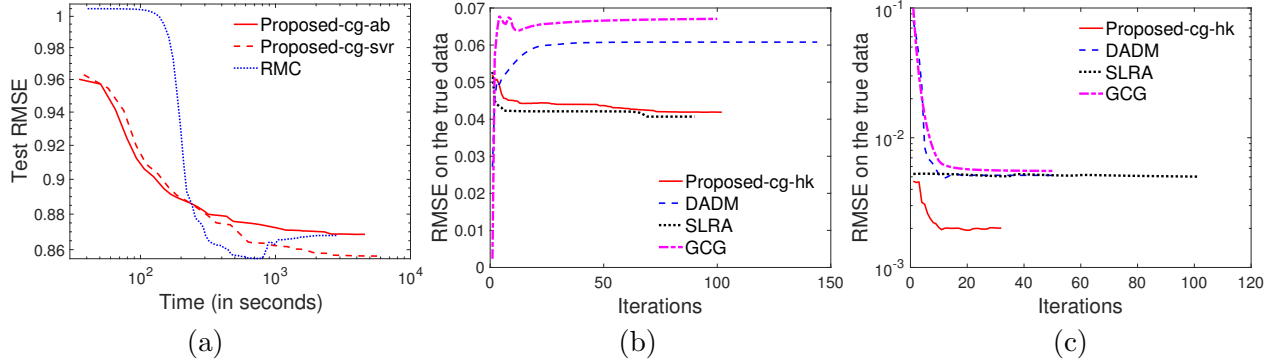


Figure A.3: (a) Evolution of test RMSE of different robust matrix completion algorithms on the Netflix data set; (b) Performance on stochastic system realization problem; (c) Performance on system identification problem;

It can be observed that Proposed-tr-sq approach the global optima for the nuclear norm regularized problem (1) in very few iterations and obtain test RMSE $\approx 2.46 \times 10^{-7}$. Our first order algorithm, Proposed-cg-sq, also achieves lower test RMSE at much faster rate compared to APGL and Active ALT. Note that similar to RTRMC, our methods are able to exploit the condition that $d \ll T$ (rectangular matrices).

Real-world data set results: We tested the methods on three real world data sets: Netflix (Recht & Ré, 2013), MovieLens10m (ML10m) and MovieLens20m (ML20m) (MovieLens, 1997). Their statistics are given in Table A.2. Figures A.2 (a)&(b) display the evolution of root mean squared error on the test set (test RMSE) against the training time on the Netflix data set for first- and second-order algorithms, respectively. Proposed-cg-sq is among the most efficient first-order method and Proposed-tr-sq is the best second-order method. We outperform both APGL and Active ALT, and both our algorithms converge to a lower test RMSE than MMBS at a much faster rate. Table A.3 reports the minimum test RMSE, averaged over ten splits, obtained by all the algorithms on three large-scale real-world data sets: Netflix, MovieLens10m (ML10m), and MovieLens20m (ML20m). Both our algorithms obtain the smallest test RMSE.

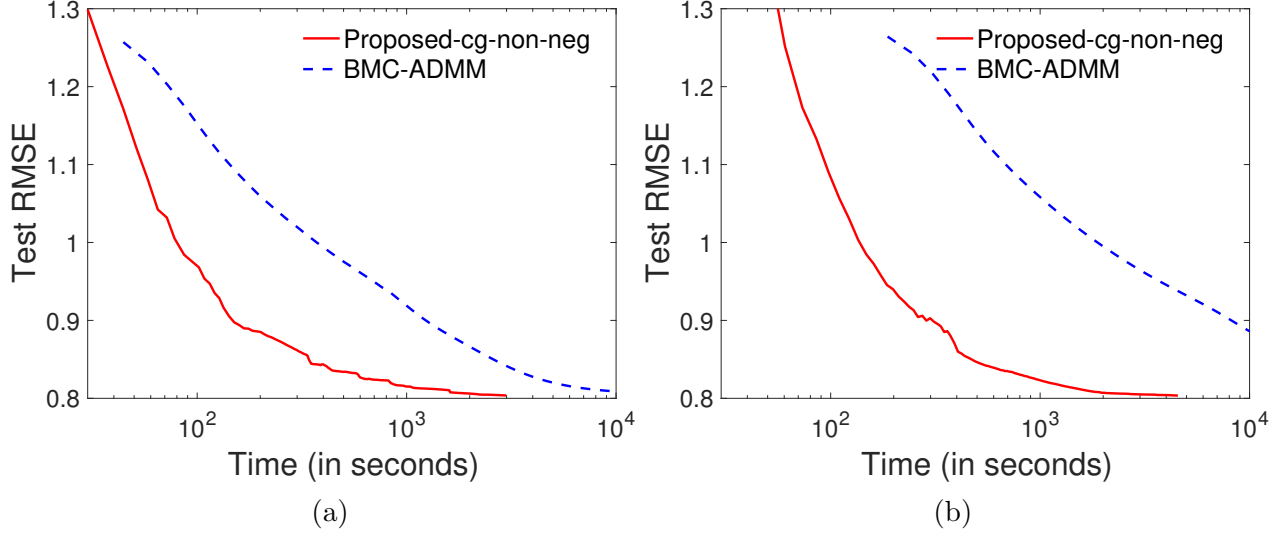


Figure A.4: Evolution of test RMSE on non-negative matrix completion problems: (a) MovieLens10m data set, and (b) MovieLens20m data set. The proposed algorithm Proposed-cg-non-neg outperforms state-of-the-art BMC-ADMM solver by an order of magnitude in MovieLens20m.

A.5.2 Robust Matrix Completion

We compare the following robust matrix completion algorithms: RMC (Cambier & Absil, 2016): state-of-the-art first-order Riemannian optimization algorithm that employs the smooth pseudo-Huber loss function (which successively approximates absolute loss), Proposed-cg-ab: our first-order algorithm with ℓ_1 -loss, and Proposed-cg-svr: our first-order algorithm employing ϵ -SVR loss. It should be emphasized that the non-smooth nature of ℓ_1 -loss and ϵ -SVR loss makes them challenging to optimize in large-scale low-rank settings. All the three loss functions are known to be robust to noise. We follow the same experimental setup described in the previous section.

Figure A.3(a) show the results on the Netflix data set. We observe that both our algorithms scale effortlessly on the Netflix data set, with Proposed-cg-svr obtaining the best generalization result. It should be noted RMC approximates ℓ_1 -loss only towards to the end of its iterations. The test RMSE obtained at convergence are: 0.8685 (Proposed-cg-ab), **0.8565** (Proposed-cg-svr), and 0.8678 (RMC), respectively.

A.5.3 Non-negative matrix completion

We compare our first-order non-negative matrix completion algorithm, Proposed-cg-non-neg, against state-of-the-art BMC-ADMM algorithm (Fang et al., 2017). BMC-ADMM has carefully designed update rules to ensure an efficient computational and space complexity. We experiment on two large-scale real world data sets: MovieLens10m (ML10m), and MovieLens20m (ML20m) (MovieLens, 1997). We run both the methods on ten random 80/20 train/test splits. The rank r for Proposed-cg-non-neg as well as the maximum rank for BMC-ADMM are set as 10. We cross-validate the regularization parameters for best performance of both algorithms.

Results: Figures A.4(a)&(b) plot the evolution of the root mean squared error on the test set (test RMSE) against the training time for both algorithms on the two data sets. We observe that our proposed algorithm Proposed-cg-non-neg is significantly faster than BMC-ADMM in converging to the best test RMSE.

A.5.4 Hankel Matrix Learning

Given the observation of noisy system output, the goal in SSR problem is to find a minimal order autoregressive moving-average model (Fazel et al., 2013; Yu et al., 2014). The order of such a model can be shown to be equal to the rank of the Hankel matrix consisting of the exact process covariances (Fazel et al., 2013; Yu et al., 2014). Hence, finding a low-order model is equivalent to learning a low-rank Hankel matrix, while being close to the given data. We perform a small and a large scale experiment in this setting.

In our first experiment, the data is generated in accordance with the setting detailed in Fazel et al. (2013); Yu et al. (2014), with $d = 21$, $T = 100$, and $r = 10$. We compare our first-order low-rank Hankel matrix learning algorithm, Proposed-cg-hk, with state-of-the-art solvers GCG (Yu et al., 2014), SLRA (Markovsky, 2014; Markovsky & Usevich, 2014), and DADM (Fazel et al., 2013). We learn a rank-10 Hankel matrix with all the algorithms. Since GCG and DADM have a nuclear norm regularization, we tune their regularization parameter to vary the rank. Proposed-cg-hk is initialized with a random \mathbf{U} matrix, SLRA’s initialization is provided by its authors, and for GCG and DADM, we initialize it with the training matrix. It should be noted that both DADM and GCG are convex approaches and their converged solutions are independent of the initialization. The best result with rank less than or equal to 10 has been reported for GCG and DADM. Figure A.3 (b) plots the variation of RMSE with respect to true data (true RMSE) across iterations. It should be noted that the training data is a noisy version of true data. We observe that our algorithm outperforms GCG and DADM and matches SLRA in terms of generalization performance. The true RMSE at convergence is: 0.0419 (Proposed-cg-hk), 0.0671 (GCG), 0.0608 (DADM) and **0.0407** (SLRA). In our second experiment, we generated the data in accordance with the setting detailed in (Markovsky, 2014; Markovsky & Usevich, 2014). We set $d = 1000$, $T = 10000$, and $r = 5$ and repeat the above experiment. The true RMSE is plotted in Figure A.3. We observe that our algorithm gives lowest true RMSE.

We also perform experiments on the airline passenger data set (Box & Jenkins, 1990). This is a time-series data set and contains the number of monthly passengers for twelve years. The seasonal variance in the number of monthly passengers possesses the Hankel structure. We learn a rank 10 Hankel matrix (with $d = 11$ and $T = 134$) corresponding to 144 data readings (y). We added Gaussian noise to y to simulate the realistic setting that the vector given to the algorithms has noise. The true RMSE obtained by SLRA, Proposed-cg-Hk, DADM, and GCG are 0.0443, 0.0506, 0.1018, and 0.0773, respectively.

A.5.5 Multi-task Learning

In this experiment, we compare the generalization performance of our multi-task feature learning algorithm Proposed-tr-mtfl (for the formulation in Table 1, row 4) with the convex multi-task feature learning algorithm MTFL (Argyriou et al., 2006, 2008). It should be stated that MTFL solves the convex problem (3) without the $\mathcal{A}(\mathbf{W}) = \mathbf{0}$ constraint optimally via an alternate optimization algorithm. Optimal solution for MTFL at different ranks is obtained by tracing the solution path with respect to parameter C , whose value is varied as $\{2^{-8}, 2^{-7}, \dots, 2^{24}\}$. We vary the rank parameter r in our algorithm to obtain different ranked solutions for a given C . The experiments are performed on two benchmark multi-task regression data sets:

- Parkinsons: We need to predict the Parkinson’s disease symptom score of 42 patients (Frank & Asuncion, 2010). Each patient is described using 19 bio-medical features. The data set has a total of 5,875 readings from all the patients.
- School: The data consists of 15,362 students from 139 schools (Argyriou et al., 2008). The aim is to predict the performance of each student given their description and earlier record.

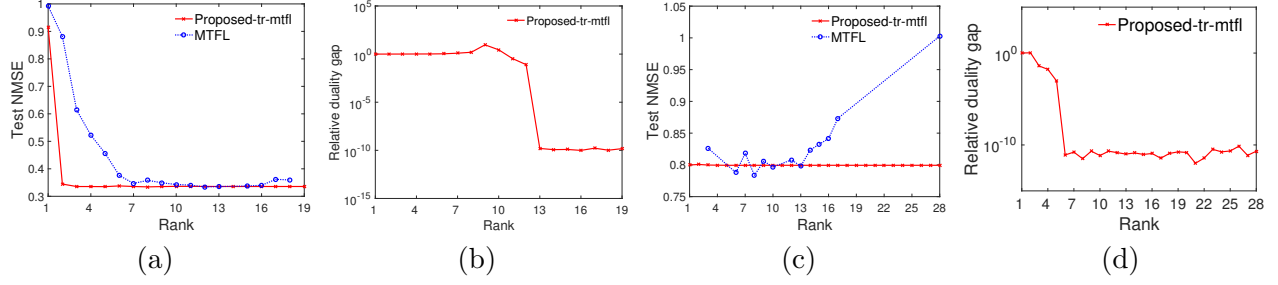


Figure A.5: (a) & (c) Variation of normalized mean squared error (NMSE) as the rank of the optimal solution changes on Parkinsons and School data sets respectively. Our multi-task feature learning method, Proposed-tr-mt, obtains best generalization at much lower rank compared to state-of-the-art MTFL algorithm (Argyriou et al., 2008); (b) & (d) The relative duality gap (Δ) corresponding to the optimal solutions obtained by our method at different ranks. A small Δ implies that our optimal solution is also the optimal solution of the trace norm regularized formulation (1). Figure best viewed in color.

Overall, each student data has 28 features. Predicting the performance of students belonging to one school is considered as one task.

Following (Argyriou et al., 2008; Zhang & Yeung, 2010), we report the normalized mean square error over the test set (test NMSE). Figures A.3 (c) present the results on the Parkinsons data set. We observe from the figure that our method achieves the better generalization performance at low ranks compared to MTFL. Similar results are obtained on the School data set.